

Georgia State University

ScholarWorks @ Georgia State University

Anthropology Theses

Department of Anthropology

12-17-2019

A COMPARISON OF MOLAR MORPHOLOGY FROM EXTANT CERCOPITHECID MONKEYS AND PLIOCENE PARAPAPIO FROM MAKAPANSGAT, SOUTH AFRICA USING ELLIPTICAL FOURIER ANALYSIS

Alexander Chil Kim*
Georgia State University

Follow this and additional works at: https://scholarworks.gsu.edu/anthro_theses

Recommended Citation

Kim*, Alexander Chil, "A COMPARISON OF MOLAR MORPHOLOGY FROM EXTANT CERCOPITHECID MONKEYS AND PLIOCENE PARAPAPIO FROM MAKAPANSGAT, SOUTH AFRICA USING ELLIPTICAL FOURIER ANALYSIS." Thesis, Georgia State University, 2019.
https://scholarworks.gsu.edu/anthro_theses/151

This Thesis is brought to you for free and open access by the Department of Anthropology at ScholarWorks @ Georgia State University. It has been accepted for inclusion in Anthropology Theses by an authorized administrator of ScholarWorks @ Georgia State University. For more information, please contact scholarworks@gsu.edu.

A COMPARISON OF MOLAR MORPHOLOGY FROM EXTANT CERCOPITHECID
MONKEYS AND PLIOCENE *PARAPAPIO* FROM MAKAPANSGAT, SOUTH AFRICA
USING ELLIPTICAL FOURIER ANALYSIS

by

ALEXANDER KIM

Under the Direction of Under the Direction of Frank L'Engle Williams, PhD

ABSTRACT

To determine whether the size and shape of *Parapapio* molars are similar to closely related cercopithecoid taxa including *Cercocebus* and *Papio* and different from more distantly related *Colobus*, three first permanent maxillary molar molds of *Parapapio* (MP77 *broomi*, MP221 *whitei*, and MP223 *whitei*) were compared to *Cercocebus agilis* (n = 11), *Papio anubis* (n = 10) and *Colobus angolensis* (n = 11) using buccolingual and mesiodistal lengths, occlusal area, and elliptical Fourier analysis. PC1, accounting for 35% of the variance, polarizes *Parapapio* and *Colobus* at opposite extremes from the other taxa, whereas PC2, explaining 19.76%, separates *Colobus* from extant cercopithecines. PC3 (13.92% of the variance) separates *Cercocebus* and *Colobus* from other genera and each other with minor overlap. In terms of shape, *Parapapio* resembles *Papio* and *Cercocebus*, but not particularly so and exhibits variation in lingual aspects of molar morphology where it resembles *Colobus*.

INDEX WORDS: Paleoanthropology, Primates, Paleontology, Dental, Molars, Papionins

A COMPARISON OF MOLAR MORPHOLOGY FROM EXTANT CERCOPITHECID
MONKEYS AND PLIOCENE *PARAPATIO* FROM MAKAPANSGAT, SOUTH AFRICA
USING ELLIPTICAL FOURIER ANALYSIS

by

ALEXANDER KIM

A Thesis Submitted in Partial Fulfillment of the Requirements for the Degree of

Masters of Arts

in the College of Arts and Sciences

Georgia State University

2019

Copyright by
Alexander Chil Kim
2019

A COMPARISON OF MOLAR MORPHOLOGY FROM EXTANT CERCOPITHECID
MONKEYS AND PLIOCENE *PARAPATIO* FROM MAKAPANSGAT, SOUTH AFRICA
USING ELLIPTICAL FOURIER ANALYSIS

by

ALEXANDER KIM

Committee Chair: Frank L'Engle Williams

Committee: Alice Gooding

Nicola Sharratt

Electronic Version Approved:

Office of Graduate Studies

College of Arts and Sciences

Georgia State University

December 2019

DEDICATION

This work is dedicated to my wonderful family, who supported me in everything I have done since my youth. Without them, I could not have achieved a tenth of what I have accomplished in my life. My mother has looked after me and has had my best interest at heart since I was born. My three younger siblings, Nick, Cody, and Hannah, have never failed to make me feel loved and I do what I do now in hope that I can be a good example to them.

I would especially like to thank my father who has remained an inspiration and example of dedication, ingenuity, and compassion throughout all my life. I inherited (not in the literal sense, of course) my scientific curiosity from him, and he has never dissuaded me from pursuing my passions. He is the role model that every young person would be lucky to have, and I am proud to call him my dad.

Last, but definitely not least, I want to thank my loving, beautiful, and smarter partner, Brooke. Brooke, you are the biggest motivation in everything that I do. I honestly do not know where I would be in life without you. Every day, you inspire me to work harder and achieve more so that I can be the partner that you deserve. I love you.

I also thank my loyal cats, Sunshower, and her sister, Sofi, who provided me companionship over many sleepless nights of graduate school.

ACKNOWLEDGEMENTS

I am grateful to my adviser and mentor, Frank L'Engle Williams, for taking me on as his student and teaching me everything I needed to be successful in my program. He is an amazing adviser whose patience and positivity enabled me to succeed in times where I otherwise may have failed. Whenever I had a personal problem or made a mistake, he was always understanding and encouraging. I will always hold him in high esteem and remember him as the person who taught me about the mentality and rigor needed to be a scientist. I hope that we continue to have a relationship as friends and colleagues for years to come.

Of course, I am thankful to my great committee members. Thank you to Dr. Alice Gooding, my undergraduate adviser, the first person to provide me with academic opportunities, and the first person who made me believe I could succeed in graduate school. Thank you, Dr. Nicola Sharratt, a genuinely thoughtful person who did not hesitate to lend me her invaluable experience and wisdom when I needed it. For contributing to my development as both an academic and person, they both stand as examples of who and what I aspire to be one day.

Thanks to Mike Raath and Phillip Tobais at the University of the Witwatersand, Johannesburg, South Africa who generously allowed access to the *Parapapio* fossils from Makapansgat in their care, and to Emmanuel Gilissen for kindly permitting the examination of extant primates at the Royal Museum for Central Africa in Tervuren, Belgium. This research was funded from grants to Frank L'Engle Williams from the Vice President for Research at Georgia State University and Fulbright-Belgium.

Thanks to the International Union for Conservation of Nature for providing the Creative Commons licensed images of Africa and the geographic distribution of the taxa (Figure 2, Figure 3, Figure 4).

Thanks to Adrian Frith for providing the Creative Commons licensed blank map of South Africa used for the creation of the cave site figure (Figure 9).

TABLE OF CONTENTS

ACKNOWLEDGEMENTS		V
LIST OF TABLES		IX
LIST OF FIGURES		IX
1 INTRODUCTION		1
1.1 Purpose of Study		1
1.2 Background of Taxa		4
<i>1.2.1 Cercopithecoid Phylogeny</i>		<i>4</i>
<i>1.2.2 Cercopithecoid Dentition and Diets</i>		<i>12</i>
<i>1.2.3 Dental Morphology and Phylogeny</i>		<i>18</i>
<i>1.2.4 Plio-Pleistocene South African Biochronology: Makapansgat and Other Cave Sites</i>		<i>21</i>
<i>1.2.5 Ecology and Morphology of Parapapio</i>		<i>23</i>
<i>1.2.6 Parapapio whitei vs. Other Parapapio</i>		<i>26</i>
<i>1.2.7 Parapapio vs. Other Cercopithecoids</i>		<i>27</i>
2 EXPERIMENT		29
2.1 Materials		29
2.2 Methods		30
<i>2.2.1 Data Collection</i>		<i>30</i>
<i>2.2.2 Elliptical Fourier Analysis</i>		<i>33</i>

2.2.3	<i>Resampling</i>	36
3	RESULTS	38
3.1	Measurements	38
3.2	Analysis	42
3.2.1	<i>Principal Components Analysis</i>	44
3.2.2	<i>Resampling and Comparison</i>	<i>Error! Bookmark not defined.</i>
4	DISCUSSION	56
4.1	Separating Taxa by Elliptical Fourier Analysis	56
4.2	Dental Morphology	56
4.3	Implications for Cercopithecoid Phylogeny	58
4.3.1	<i>Procerocebus and Parapapio</i>	58
4.3.2	<i>Parapapio species: one, two, three?</i>	59
5	CONCLUSION	61
	REFERENCES	63

LIST OF TABLES

Table 1 First and second trials for the measurements of the taxa, as well as specimen labels.	38
Table 2 Comparison of means for the measurements made on the first maxillary molars of the taxa. These taxa are morphologically distinct in size, as is reflected in the differences in their molar measurements.	39
Table 3 The differences between the first and second set of measurements performed for the measurement error analysis were not found to be significant.....	39
Table 4 ANOVA results across taxa.	40
Table 5 Tukey's Test between taxa. All measurements resulted in significantly different means between taxa except for the area measurements between <i>Cercocebus</i> and <i>Colobus</i> , and <i>Papio</i> and <i>Parapapio</i>	40

LIST OF FIGURES

Figure 1 Primate cladogram, not to scale. <i>Papio</i> and <i>Cercocebus</i> are the closest related taxa, followed closely by <i>Parapapio</i>	2
Figure 2 Map of <i>Cercocebus agilis</i> geographic distribution. Agile mangabeys are largely concentrated in the forests of Central Africa. Image courtesy of the International Union for Conservation of Nature.	6
Figure 3 Map of geographic distribution of <i>Papio anubis</i> . Olive baboons are widely dispersed across the forests and savannah plains of Central Africa and intermittently in parts of the Sahara Desert. Image courtesy of the International Union for Conservation of Nature.	7

- Figure 4 Map of geographic distribution of *Colobus angolensis*. It is found primarily in the Congo basin, though there are populations in East African Kenya and Tanzania. Image courtesy of the International Union for Conservation of Nature. 8
- Figure 5 A binarized image of the occlusal surface of the maxillary first molar of MP77 *Parapapio broomi* sided and labeled with the four cusps..... 12
- Figure 6 The maxillary dental arcade of *Cercocebus agilis* RG 8381, exhibiting the large canines and bilophodont molars typical of cercopithecids. 15
- Figure 7 The maxillary dental arcade of *Papio anubis* RG 18471. The teeth of *Papio* are significantly larger in size than *Cercocebus* or *Colobus*, but closely resemble *Cercocebus* in shape. 16
- Figure 8 The maxillary dental arcade of *Colobus angolensis* 10539. While similar to *Cercocebus* in size, the molars of *Colobus* are arranged in rows connected by ridges that help process tough leaves. 17
- Figure 9 A map of South African cave sites where *Parapapio* has been found. *Parapapio antiquus* specimens from Taung are now under consideration for being reclassified as a new genus, *Procercocebus*, due to morphological similarities to *Cercocebus torquatus* (Gilbert 2007). Original map image is courtesy of David Frith. 20
- Figure 10 Two examples of *Parapapio whitei* dentition. MP223 (top) and MP 221(bottom) derive from Makapansgat cave, South Africa, dated using biochronology to 2.9 Ma (Williams, 2014). The left first molar of MP 223 is too damaged for occlusal surface measurements..... 24

- Figure 11 A fractured maxilla from MP77, considered to be *Parapapio broomi* from Makapansgat cave, South Africa 2.9 Ma. *Parapapio* species are distinguished by size as they possess similar molar morphologies. 25
- Figure 12 Example of a *Parapapio*, *Cercocebus*, and *Papio* occlusal outline that would be used in elliptical Fourier analysis. After measurements are taken of the molar, the occlusal outline image is binarized to capture the shape for the analysis. *Parapapio* and *Papio* molars are up to three times as large as some *Cercocebus* molars, but the binarized images are scale independent because elliptical Fourier analysis captures shape rather than size. 32
- Figure 13 An example of Procrustes superimposition for elliptical Fourier analysis. The binarized molar image is reduced to the shape of the occlusal surface outline and imposed over the ellipse. The differences between the ellipse and the molar shape create the mathematical description for the principal components analysis. 33
- Figure 14 The linear regression of the mesiodistal and buccolingual measurements taken from the first trial. *Cercocebus* and *Papio* are primarily above the regression line, while *Colobus* is mostly below the regression line. *Parapapio* specimens display a normal dispersion. 41
- Figure 15 Visualization and graph of contrasting PC 1 and PC 2. 1 represents *Cercocebus*, 2 represents *Colobus*, 3 represents *Papio*, and 4 represents *Parapapio*. 44
- Figure 16 Visualization and graph of contrasting PC 3 and PC 4. 1 represents *Cercocebus*, 2 represents *Colobus*, 3 represents *Papio*, and 4 represents *Parapapio*. 46
- Figure 17 Visualization and graph of contrasting PC 5 and PC 6. 1 represents *Cercocebus*, 2 represents *Colobus*, 3 represents *Papio*, and 4 represents *Parapapio*. 48

Figure 18 Graph of resampled PC1 and PC2. *Papio* and *Cercocebus* are closely grouped;

Cercocebus is also the taxon in closest proximity to *Parapapio*..... 50

Figure 19 Graph of resampled PC3 and PC4. *Parapapio* and *Colobus* are grouped here, while

Papio and *Cercocebus* are now separated. *Cercocebus* aligns with *Parapapio* and

Colobus on PC4, while *Papio* is closer to *Parapapio* and *Colobus* on PC3. 52

Figure 20 Graph of resampled PC5 and PC6. *Parapapio* clusters with *Papio* on PC5 and with

Cercocebus and *Colobus* on PC6. *Colobus* and *Cercocebus* are grouped on both PC5 and

PC6..... 54

1 INTRODUCTION

1.1 Purpose of Study

In the study of extinct primates, anthropologists are often relegated to using limited and damaged fossil remains. This poses challenges for the classification of extinct taxa, as well as complicating the ability to establish the evolutionary relationship of fossil specimens to extant taxa. In many cases, the paleontological evidence is limited to fossilized fractured bone elements and teeth. Fortunately, teeth are among the most informative skeletal remains, often providing insight into body size, differences between sexes, dietary proclivities, and the environment that these taxa inhabited. As mammals, primates possess heterodont teeth that differ from front to back, rather than possessing teeth of one variety like many reptiles and fish. Of these teeth, the molars are particularly informative because primates rely on them to process a variety of foods, and as a consequence, molars are under heavy selective pressures and evolve rapidly as taxa radiate into new environments and fill different niches. In current primate phylogenetics, there is an abundance of fossil material relating to cercopithecoid monkeys, though many questions remain about the evolutionary history of extant taxa like *Cercocebus* and *Papio* to fossil taxa like *Parapapio*. While *Parapapio* teeth are found across a variety of South African sites, anthropologists still struggle to differentiate *Parapapio* species. Furthermore, the relationship of *Parapapio* to other cercopithecoid monkeys is a changing landscape, with new genera being named as recently as 2007 (Gilbert 2007). The purpose of this study is twofold: to test a method of separating primate taxa by the occlusal shape of their molars, and to look for new insights into the existing relationships of cercopithecoid monkeys.

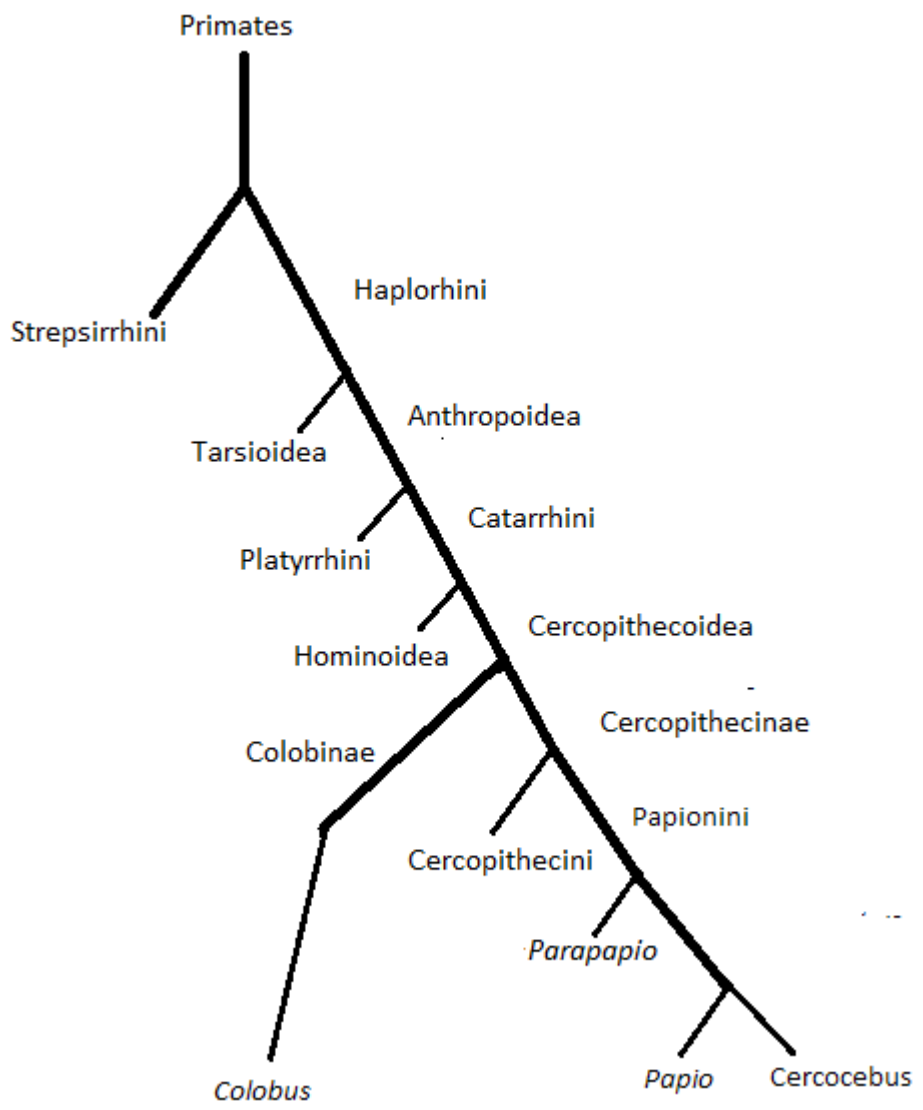


Figure 1 Primate cladogram, not to scale. *Papio* and *Cercocebus* are the closest related taxa, followed closely by *Parapapio*.

It is the goal of this research to examine the similarity in size of *Parapapio* to *Cercocebus* and *Papio*, and investigate the occlusal molar shape of these taxa, as well as outgroup *Colobus* using elliptical Fourier analysis. Elliptical Fourier analysis can provide insight into how these different taxa diversified, even in the absence of postcranial remains, by comparing and contrasting the shape of the molars without the variable of size. Considering the heritability of molar morphology, the results of the analysis should support the established phylogeny and reflect that *Papio* and *Cercocebus* resemble one another more closely than the other taxa due to a more recent evolutionary divergence, followed by *Parapapio*. These three taxa should be more similar to each other than any are to *Colobus*.

By measuring and comparing the differences in molar surface shape, it is possible to extrapolate the phylogenetic relationships of these taxa as they radiated into different dietary niches and ecosystems, with closely related taxa being similar when compared to more divergent taxa. Crown area measurements are not recommended for phylogenetic analysis, as it has been found to be highly variable depending on sex, body size, and subspecies, explaining between 34 to 42% of the crown area difference in baboons (Hlusko et al. 2002). However, analysis of the shape of the molar occlusal surface as an indicator of phylogenetic relationships is less explored. The shape of the occlusal surface consists of the size and placement of the cusps relative to one another. Previous research on the heritability of molar cusp size in baboons has found that mandibular molar cusp size is heritable and highly linked to genetic expression, explaining between 15 to 42% in at least one population of baboons (Hlusko et al. 2006). While the M_1 was not found to be more heritable than the second or third molars, it does show higher genetic correlations, meaning that the M_1 is less prone to phenotypic variation but retains a strong

relationship with other genetic expressions (Hlusko et al. 2006). Furthermore, studies on cranial and postcranial variation in catarrhine skeletons have shown that what intraspecific variation exists is reduced in the cranium compared to the postcranial skeleton (Buck et al. 2010).

Elliptical Fourier analysis can be utilized to test hypotheses relating to morphology and shape, with the exclusion of size as a variable. Some hypotheses focusing on the evaluation of morphological variation between taxa that exhibit a large range of sizes might use elliptical Fourier analysis to compare shapes of anatomical features. For the analysis of extinct taxa, affinity could possibly be examined through a comparison of shape, where multiple taxa exhibit ancestral and derived characteristics but vary in size. These differences in shape can help to determine numerous morphological characteristics of extinct taxa, such as foraging or dietary preferences.

1.2 Background of Taxa

1.2.1 Cercopithecoid Phylogeny

In the order Primates, the suborders are split into Strepsirrhini, the lemurs, pottos, and lorises, and Haplorhini, where the tarsiers, monkeys, and apes are placed. The Catarrhine parvorder of Haplorhini contains the Old World monkeys and apes (Szalay and Delson 1979). The Cercopithecidae family of monkeys are the most abundant in the world, being widely distributed across various ecological niches in the African and Asian continents, with limited presence in Europe. The cercopithecids consist of two subfamilies: the Cercopithecinae and Colobinae. These subfamilies include twenty extant genera between them. Differences in dentition and diet are among the major characteristics separating the two subfamilies, as well as differences in habitat, locomotion, social organization, and size. The Cercopithecidae originated

sometime in the late Oligocene to early Miocene and rapidly expanded in diversity by the late Miocene to early Pleistocene (Strasser and Delson 1987). Molecular studies on the phylogeny of the Cercopithecoidea place the divergence of the Cercopithecinae and Colobinae at approximately 19.4 million years ago (Monson and Hlusko 2014). The Papionini tribe, which includes both *Papio* and *Cercocebus*, separated from Cercopithecini around 7 million years afterwards. The papionins exhibit longer faces with wide nasal breadth and an affinity for terrestrial environments. Cercopithecini is defined by three synapomorphies that separates them from the ancestral morphotype. The first is the absence of the hypoconulid on the third lower molar. The molar flare that creates the pointed molar shape is also reduced. Finally, there is a fragmented dispersion of diploid numbers in cercopithecins, ranging from 48 to 72, compared to the 42 in all papionins and 44 in most colobines (Szalay and Delson 1979).



Figure 2 Map of Cercocebus agilis geographic distribution. Agile mangabeys are largely concentrated in the forests of Central Africa. Image courtesy of the International Union for Conservation of Nature.

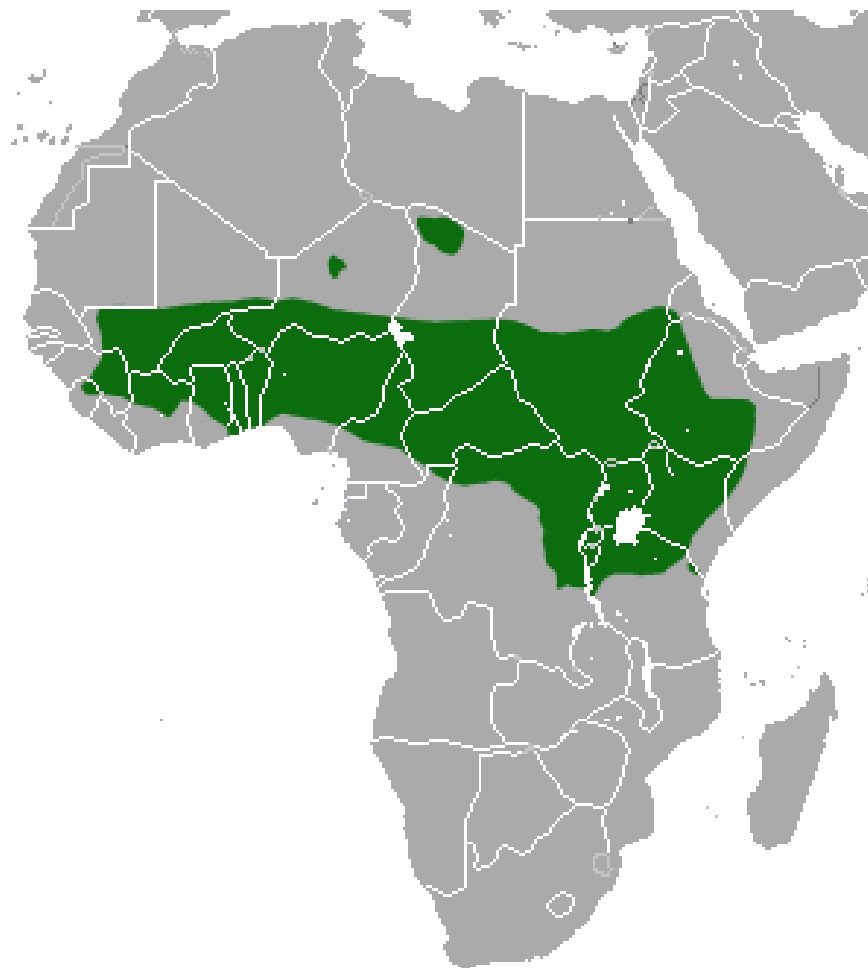


Figure 3 Map of geographic distribution of Papio anubis. Olive baboons are widely dispersed across the forests and savannah plains of Central Africa and intermittently in parts of the Sahara Desert. Image courtesy of the International Union for Conservation of Nature.



Figure 4 Map of geographic distribution of Colobus angolensis. It is found primarily in the Congo basin, though there are populations in East African Kenya and Tanzania. Image courtesy of the International Union for Conservation of Nature.

It has been suggested that the emergence of the papionin subtribes can be traced back to the expansion of the Sahara Desert, sometime in the late Miocene between 9 and 6 million years ago (Strasser and Delson 1987). It was around this time that papionins likely began exploiting the terrestrial spaces of the woodland and savannah environments. These new terrestrial forms would have had an easier time crossing the Sahara Desert than the arboreal taxa. Eventually, the Sahara Desert would have become too deadly of an obstacle for further dispersion, limiting the gene flow of papionins and rendering them as two separated populations. The population to the north of the desert, probably the founding population of macaques, spread westward and radiated across Europe and Asia, while the southern population radiated through the rest of Africa as the ancestors of baboons, geladas, and mangabeys (Szalay and Delson 1979). The Sahara remains a large environmental barrier for many cercopithecoid monkeys, containing many extant taxa to central and southern Africa (Figure 2; Figure 3; Figure 4).

Still, there are no derived traits yet described to adequately characterize North African and Eurasian Macacina, and sub-Saharan Papionina. Extinct and extant *Macaca* are easily distinguishable from African papionins as a genus due to the retention of ancestral morphology, specifically the facial shape, absence of facial fossae, and locomotor adaptations. There are extinct genera of macaques found in Eurasia that seem to exhibit derived traits for terrestrial locomotion, but these characteristics are not found in any extant macaques (Strasser and Delson 1987).

Theropithecus is the most derived of all the papionins and exhibits several autapomorphies of the cranial and postcranial skeleton that make it unique from the others. These numerous distinctions have raised questions about the phylogeny of *Theropithecus* and lead some to consider reclassifying it as a sister-taxon to papionins (Strasser and Delson 1987).

The earliest known *Theropithecus* fossils place the taxon as being at least 4 million years old, potentially resulting in millions of years to acquire its autapomorphies. *Papio* and *Theropithecus* are not unique in their need for elaboration. *Cercocebus* and *Mandrillus* were once controversial in their respective placements, with *Cercocebus* grouped with *Lophocebus* and *Mandrillus* grouped with *Papio*, but they have since been clarified as belonging to their own clade, separate from the baboons and macaques (Gilbert et al. 2009).

Cercopithecini is relatively less skeletally diverse across taxa, which makes it difficult to discern phylogenetic relationships between members. In addition to *Cercopithecus*, there are three other genera: *Allenopithecus*, *Erythrocebus*, and *Miopithecus*. *Allenopithecus* seems to retain many of the ancestral traits lost or reduced in other cercopithecines, including the molar flare, continuous ischial callosities on males, and estrus swelling in females. It also has the lowest diploid count out of any of the Cercopithecini. Altogether, the differences between *Allenopithecus* and the other Cercopithecini are equivalent to the differences between Papionini and the colobines. Because of these differences, it has been suggested that *Allenopithecus* is removed from Cercopithecini and placed into its own subtribe: Allenopithecina (Strasser and Delson 1987). *Miopithecus* faces similar scrutiny, due to females undergoing color changes of the sexual skin, but the presence of the other traits associated with Cercopithecini makes their separation unlikely. *Erythrocebus* is unique from the other two genera in that it is the most distinct genus of them all in terms of skeletal morphology but does lack the cyclical coloration of the sexual skin. Because *Miopithecus* and *Erythrocebus* are so distinct from *Cercocebus* and both have a low diploid number of 54, it is likely that the two genera separated from *Cercopithecus* very early in its evolutionary lineage (Strasser and Delson 1987).

Fossil colobines are common between the late Miocene and throughout the Plio-Pleistocene, but their exact relationship to the modern lineages of colobines is still uncertain. Despite an abundance of fossil material available for African colobines, representing at least six distinct genera, the phylogenetic relationship between the extinct and extant taxa remains to be clarified (Frost et al., 2015). Many colobine fossils are heavily fragmented, and cranial fragments are rare. For these reasons, they are assigned to genus *Colobus* until more evidence has been described (Szalay and Delson 1979). Isotopic signatures from *Cercopithecoides williamsi* seem to agree with a diet based predominantly on C₄ plants like grasses, while dental microwear suggests grasses as well as underground storage organs were consumed (Williams and Geissler 2014). Morphological traits that might indicate semi-terrestrial locomotion have been explained as being potentially derived from arboreal ancestors. It is characterized by the significant reduction of the first metacarpal, a trait that it shares with the African colobines, and to a lesser extent, the rest of Colobinae. It is possible that the last common ancestor of all the colobines was a brachiator and used suspensory locomotion to navigate the forest environment. The reduction of the first metacarpal in *Cercopithecoides williamsi* is equivalent to extant African colobines, making it the earliest known example of colobine thumb reduction in the fossil record (Frost et al., 2015). Fossil colobines from Asia like *Mesopithecus* lack the reduced thumb, indicating that the reduction of the thumb in African and Asian colobines are examples of convergent evolution, as is the diminutive pollical digit of semi-brachiating large platyrrhines. *Cercopithecoides williamsi* was a contemporaneous species with *Parapapio*, and these morphological and isotopic differences reflect niche divergence within a shared ecology and highlight the emerging dietary and evolutionary divergence of cercopithecoid monkeys as early as the middle Pliocene.

1.2.2 Cercopithecoid Dentition and Diets

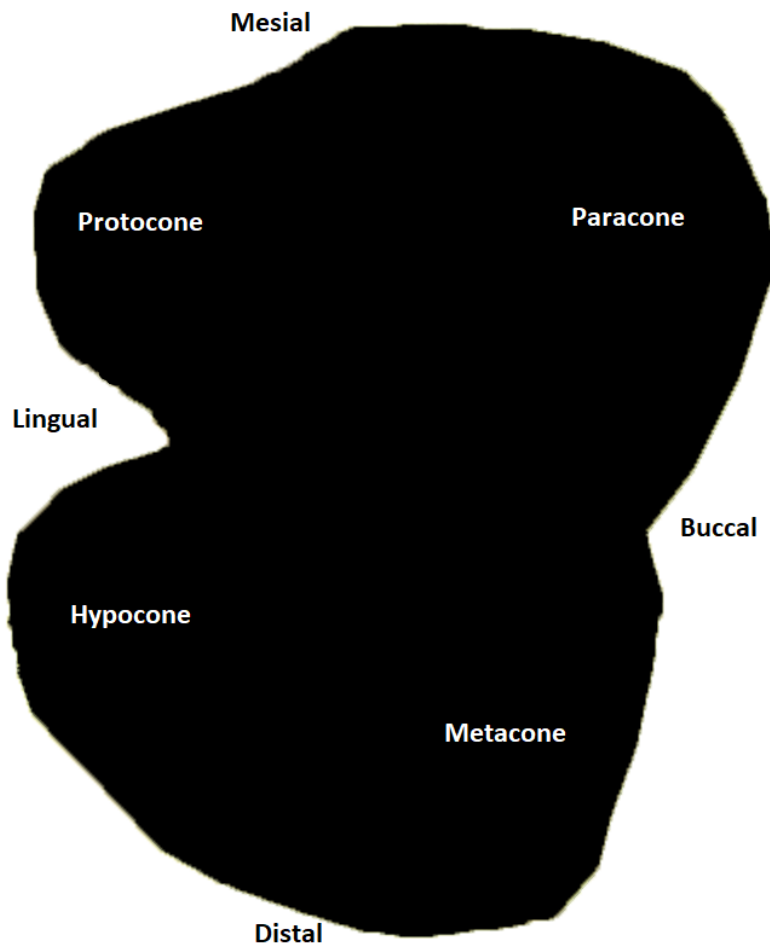


*Figure 5 A binarized image of the occlusal surface of the maxillary first molar of MP77 *Parapapio broomi* sided and labeled with the four cusps.*

The dental morphology of primates can vary widely across taxa, but cercopithecids do share several traits. All cercopithecids have a dental formula of two incisors, one canine, two premolars, and three molars per quadrant of the dental arcade, frequently represented as 2-1-2-3. Although cercopithecoid monkeys have the same number of teeth, the shapes and sizes of these teeth are distinct between taxa as a result of different factors influencing their evolution over millions of years, such as diet, sexual selection, or social displays involving the teeth, specifically the canines. The molars of cercopithecids are bilophodont, consisting of four to five cusps arranged in two separate rows. In all cercopithecoid monkeys, the four maxillary cusps are the paracone, protocone, metacone, and hypocone. It is the loph-guided occlusion produced by these cusps that enable cercopithecids to process the foods that they do (Monson and Hlusko 2014). All cercopithecoid monkeys make heavy use of their molars for food processing because their diets are largely comprised of hard and tough food objects, such as nuts, roots, leaves, fruit, and other plant matter. Cercopithecinae are typically more generalist consumers, while the Colobinae exhibit highly folivorous diets. These differences in diet are represented by three extant genera: *Cercocebus*, *Papio*, and *Colobus*. These genera are distinct in their diets, engaging in durophagy, omnivory, and folivory, respectively, with the molar morphology and shape of their molars varying accordingly.

While cercopithecines and colobines share numerous dental characteristics, there are several that are effective in distinguishing the subfamilies. Cercopithecines have buccal cheek pouches for the storage of foods that are absent in colobines, which instead rely on specialized stomachs to process their folivorous diet. Cercopithecines also have specialized incisors, in contrast to their molars which retain the ancestral condition. *Papio* in particular exhibits a high degree of sexual dimorphism that extends to the canines, which are much larger in males for

display and fighting purposes. In contrast, compared to the retention of ancestral molar characteristics in cercopithecines, the shape of colobine molars is very dissimilar to *Cercocebus* and *Papio*. The molar relief present in colobines is intensified, creating high cusps with notches in the tooth wall that assist in the shearing and processing of leaves. This characteristic also independently arose in *Theropithecus*, indicating that it is likely strongly selected for in monkeys that process a lot of tough plant matter (Strasser and Delson 1987).



Figure 6 The maxillary dental arcade of Cercocebus agilis RG 8381, exhibiting the large canines and bilophodont molars typical of cercopithecids.



Figure 7 The maxillary dental arcade of Papio anubis RG 18471. The teeth of Papio are significantly larger in size than Cercopithecus or Colobus, but closely resemble Cercopithecus in shape.



Figure 8 The maxillary dental arcade of Colobus angolensis 10539. While similar to Cercocebus in size, the molars of Colobus are arranged in rows connected by ridges that help process tough leaves.

1.2.3 *Dental Morphology and Phylogeny*

The definitive dental characteristic of cercopithecids are their “cheek teeth.” The ancestral cercopithecoid taxon is recognized by the absence of the hypoconulid, leading to the bilophodont arrangement of cusps seen in all cercopithecoid taxa (Szalay and Delson 1979). Bilophodont molars are best suited for slicing tough foods, indicating that early cercopithecoids were dependent on leaves for at least part of their diet (Figure 6; Figure 7; Figure 8). Another adaptation of cercopithecoids was the incorporation of the buccal cingula on the lower molars into the tooth wall, creating a wide base for the molars that narrows at the top, which is ideal for the processing of leaves (Strasser and Delson 1987). This characteristic is most prominent in extant taxa, with extinct taxa exhibiting reduced instances of this absorption represented by the presence of a small but visible cingulum. Additionally, the canines of cercopithecoids are sexually dimorphic and larger in size compared to the other teeth (Szalay and Delson 1979). In males, the upper canines possess a deep cleft on the mesial surface that runs to the root (Szalay and Delson 1979). To sharpen these canines, cercopithecoids use the honing complex located along their P₃ that extends to the alveolar surface of the bone, which provides greater surface area for sharpening compared to the obliquely-angled space that exists in ancestral taxa (Strasser and Delson 1987). These dental traits are ubiquitous in cercopithecoids and can be used to trace cercopithecoid phylogeny back to the early eucatarrhines.

Cercocebus and *Papio* also both exhibit a relatively unique feature on the lingual side of the maxillary molars called an interconulus. The interconulus is sometimes referred to as a lingual cingulum or lingual conule. It is located between the protocone and hypocone and varies in size and shape. Sometimes it is present as a small divot, and other times it is expressed as a large cingulum (Monson and Hlusko 2014). This trait is believed to be a lingering remnant of the

lingual cingulum found in early mammalian dentition. It is possible that this trait is created by the same processes that developed the lingual cusps, with the expression being tied to bilophodonty and the spacing of the cusps (Monson and Hlusko 2014). The main argument in favor of this interpretation is the distinctive shape and placement of the interconulus, which is located between the mesial and distal lophs and appears to only occur in bilophodont molars (Monson and Hlusko 2014). Cercopithecins and colobines have both lower rates of expression, and diminished expression when the interconulus is present. The high frequency of the interconulus in papionins compared to other taxa has been suggested to be a derived trait, and possibly an identifying characteristic of papionins evolving in the Miocene (Monson and Hlusko 2014).



Figure 9 A map of South African cave sites where *Parapapio* has been found. *Parapapio antiquus* specimens from Taung are now under consideration for being reclassified as a new genus, *Procerocebus*, due to morphological similarities to *Cerocebus torquatus* (Gilbert 2007). Original map image is courtesy of David Frith.

1.2.4 Plio-Pleistocene South African Biochronology: Makapansgat and Other Cave Sites

South African cave sites are abundant in papionin fossil deposits, specifically those assigned to *Parapapio*, which have been found in great numbers across multiple different localities like Sterkfontein, Taung, and Makapansgat (Figure 9). The karstic elements of these cave sites have complicated efforts to date them through stratigraphic sequencing. Paleomagnetic dating places both Sterkfontein and Makapansgat as originating in the Pliocene. This is upheld by faunal analysis that places Makapansgat and Sterkfontein as the most similar in the distribution of taxa (Williams et al. 2007; Williams and Geissler 2014). Some sites like Taung are dated primarily through comparisons of faunal fossil deposits to other such assemblages (Williams and Patterson 2010). Paleoenvironmental reconstructions have been created from a variety of different methods, including analysis of macrobotanical remains and pollen. These reconstructions generally agree that early sites like Makapansgat and Sterkfontein were more heavily wooded compared to the open environments of later sites (Reed 1997). Makapansgat reconstructions also suggest a sudden change from an open environment dominated by grasses and shrubs to extensive tree cover surrounding the area. Later, the open environment would partially return to create a diverse habitat consisting of valleys and plains (Reed 1997).

Extensive work has been done using papionin fossils and their morphological characteristics as biochronological indicators, giving insight into the shifting environment and ecology of Plio-Pleistocene South Africa. Biochronology is distinct from biostratigraphy in its emphasis on an external dating source in the comparison of two faunal assemblages, one dated and one undated (Williams et al., 2007). With the exception of Swartkrans, *Parapapio* and fossil *Papio* are strongly associated with differing cave sites and time frames, which is the predominant reason they are used as temporal indicators. Biochronology estimates place the age of the

Makapansgat fossil deposits at approximately 3.03 to 2.58 million years ago, though magnetobiostratigraphy places it as being closer to 2.85 million years.

Isotopic analysis of Makapansgat *Parapapio* shows that their diets were heavy in both C₃ and C₄ vegetation, which is consistent with paleoecological reconstructions as mosaic forest habitats (Codron et al. 2005). Though they likely consumed a variety of plant foods, their molar morphology and C₃ signal does indicate a diet heavy in frugivory. Much like modern baboons, though, *Parapapio* has shown regional variation in diet between South and East African sites. South African *Parapapio*, like the ones found at Makapansgat, would have been more folivorous than their East African counterparts. These same dietary patterns are generally reflected in the extant *Papio* of South Africa, *Papio hamadryas*, with one notable exception: grasses. *Parapapio* from South Africa consumed considerably more grasses or grassroots of C₄ plants than both their contemporaries from East Africa and extant *Papio*, at levels exceeding some grazing ungulates from the same sites (Codron 2005).

The smaller size of *Parapapio* is a quality it shares with other ancestral papionin primates and serves to validate the age estimation of cave sites like Sterkfontein, Makapansgat, and Taung, where it is present. Conversely, the larger-bodied fossil papionins like *Papio* and *Theropithecus* are more commonly found in Pleistocene cave deposits (Williams et al., 2007). Similar to the differences in size, differences in degrees of sexual dimorphism can also be used as indicators of biochronology between the taxa. *Parapapio* exhibits significantly reduced sexual dimorphism compared to that seen in more recent papionins, most notably in the enhancement of facial prognathism of males. While the differences between *Parapapio* and other fossil papionins are largely understood, there is still much to be clarified about the phylogeny of the different *Parapapio* species.

1.2.5 Ecology and Morphology of *Parapapio*

To understand the divergence of early cercopithecids across their numerous ecological niches, it is necessary to examine the relationship of ancestral taxa like *Parapapio* with the biochronology of Plio-Pleistocene periods. Beginning in the Miocene, cercopithecoid monkeys began to radiate out of northern and central Africa into southern parts of Africa, where *Parapapio* fossils are found in abundance, along with fossils belonging to other extinct cercopithecoid monkeys. The dietary and environmental flexibility of the early papionins was critical to the radiation of the taxa as many became more terrestrial to utilize resources uncontested by other primates of the time, such as seeds, bark, and underground storage organs (Williams and Patterson 2010).

The absence of postcranial remains for many *Parapapio* species makes estimations of their skeletal morphology difficult to ascertain. At the Cradle of Humankind World Heritage site, located Bolt's Farm in South Africa, excavations did yield *Parapapio* postcranial remains consisting of a humerus, femur, and patella (Gommery et al., 2008). The bones exhibit definite cercopithecoid qualities like those seen in papionins. The bones are robust, indicating a preference for either terrestrial or semi-terrestrial locomotion. Associated microfauna show evidence of a dry, open environment similar to plainlands (Gommery et al., 2008). These postcranial structures likely differ in some qualities compared to *Parapapio* of sites like Makapansgat, known for being more heavily forested at times.



Figure 10 Two examples of Parapapio whitei dentition. MP223 (top) and MP 221(bottom) derive from Makapansgat cave, South Africa, dated using biochronology to 2.9 Ma (Williams, 2014). The left first molar of MP 223 is too damaged for occlusal surface measurements.



Figure 11 A fractured maxilla from MP77, considered to be Parapapio broomi from Makapansgat cave, South Africa 2.9 Ma. Parapapio species are distinguished by size as they possess similar molar morphologies.

1.2.6 *Parapapio whitei* vs. Other *Parapapio*

It can be difficult to discern between the species of *Parapapio* due to limited postcranial remains in sub-Saharan Africa, as well as conflicting isotopic data and measurements that seem to indicate that different species might instead be sexually dimorphic specimens of the same species, as illustrated by research using these isotopic and metric analyses finding *Parapapio jonesi* overlaps with female *Parapapio broomi* (Gommery et al., 2008; Figure 11). There are some morphological differences between East African and South African *Parapapio* found in the dentition, specifically the molars. Comparisons of these three traits between the East African and South African taxa show greater reliance on frugivorous diets in the East African taxa, with South African taxa engaging in greater degrees of folivory at earlier sites. In contrast to other *Parapapio* species of the time, *Parapapio whitei* was significantly less frugivorous, eating the least fruit out of all three taxa. The cranium and molar size of *Parapapio whitei* is also the largest of all *Parapapio*. Larger facial features seem to suggest that *Parapapio whitei* might have been a more terrestrial, large-bodied species, but no postcranial remains have ever been found in South African deposits, so this remains to be confirmed (Figure 10). Body size estimates derived from dental proportions support this hypothesis (Delson 2000). Dental microwear from Makapansgat shows a greater abundance of pits in the molars, likely the result of foraging for gritty underground food sources (Williams 2014). Similar microwear analysis performed on *Parapapio whitei* also shows increased consumption of underground storage organs, perhaps as a necessary adaptation to maintain the caloric intensity of larger body sizes. Additionally, it is possible that the abundance of C₄ foods at Makapansgat required *Parapapio whitei* to ingest higher amounts of grit in its diet from the consumption of underground storage organs compared to *Parapapio* of more forested regions like Sterkfontein (Williams 2014).

1.2.7 *Parapapio* vs. *Other Cercopithecids*

The phylogenetic relationships of cercopithecids are largely understood, but recent studies utilizing molecular and morphological data portray a more complex evolutionary landscape than originally perceived. *Parapapio* is almost certainly a paraphyletic group that contains the stem African papionins, or perhaps just the clade of *Papio*, *Lophocebus*, *Rungwecebus*, and *Theropithecus* (Pugh and Gilbert 2018). *Theropithecus* is considered basal to this clade, having diverged from the rest of the clade approximately 4 to 5 million years ago (Pugh and Gilbert 2018). One species of *Parapapio*, *Parapapio antiquus*, considered the stem taxon in the emergence of the *Cercocebus* and *Mandrillus* clade, or at least basal to *Mandrillus*, was reclassified as a sister genus, *Procercocebus*. Evidence for this new taxon includes craniodental similarities shared with some *Cercocebus* taxa, like *Cercocebus torquatus*, and postcranial similarities shared with *Mandrillus*, specifically in the robust humerus and strong muscle markings (Gilbert 2007; Pugh and Gilbert 2018).

Many cercopithecoid fossils from the Plio-Pleistocene show an inclination for terrestrial behavior and feeding (Williams 2014). By the Pliocene, some Cercopithecinae, namely *Theropithecus*, were already heavily adapted for eating grasses, and taxa found in open and closed environments seem to point to the utilization of both terrestrial and arboreal environments. *Parapapio* was likely one of these genera exploiting both the ground and the trees as a source of food, as seen in the C₃ and C₄ isotopic signatures of these animals (Fourie et al., 2008). *Parapapio* appears to have eaten a lot of vegetative matter close to the ground. This is further supported by the dental microwear, which separates Pliocene *Parapapio* from extant taxa found in tropical forests. Compared to extant taxa, which rely heavily on hard object foods, molars of extinct South Africa taxa exhibit lower pit percentages and smaller pit size and depth

(El-Zaatari et al., 2005). Analysis of dental microwear patterns in eight extinct cercopithecoid species from cave sites including Makapansgat, Sterkfontein, and Swartkrans show gradual changes in the dietary proclivities of some species in adaptation to their immediate environments. *Parapapio jonesi* from Makapansgat ate a diet consisting almost entirely of grasses or leaves, while *Parapapio jonesi* from Sterkfontein exhibit microwear associated with a diet of grasses, leaves, and other hard foods (El-Zaatari et al., 2005). Because of the differences exhibited in microwear between individuals of the same species and similar times, some caution should be exercised when attempting to reconstruct paleoecology from microwear alone.

The examination of molar shape and morphology by elliptical Fourier analysis could prove to be a reliable resource in the study of primate phylogenetics. Molar morphology is highly heritable and reflected in the shape of the occlusal surface, where the molar cusps are located. While *Parapapio* shares some dietary affinities with *Colobus*, it is a closer relative to *Papio* and *Cercocebus*. Additionally, *Parapapio* and *Papio* are larger in size than *Cercocebus* and *Colobus*. Because they are closely related taxa, the elliptical Fourier analysis should place *Cercocebus* and *Papio* closer together with the exclusion of *Colobus*, while *Parapapio* is placed on its own but closer to the cercopithecines than with *Colobus*.

EXPERIMENT

1.3 Materials

Measurements and images were taken from 35 total specimens of four different genera using epoxy resin dental casts of the first permanent maxillary molar casted by Frank Williams and provided by the Williams Dental Cast Collection at Georgia State University (Williams et al. 2007; Williams 2014). The casts of the extant taxa were originally created at the Royal Museum of Central Africa in Tervuren, Belgium (Figure 10). The fossil specimens were cast courtesy of the Department of Anatomical Sciences at the University of the Witwatersrand Medical School in Johannesburg, South Africa. When selecting specimens, it is important to avoid those with significant occlusal damage or casting errors, as these problems can affect the accuracy of the results. The four taxa measured were *Cercocebus agilis* (n = 11), *Papio anubis* (n = 10), *Colobus angolensis* (n = 11), and *Parapapio* (n = 3). Originally, 30 additional specimens were included, but were eventually removed due to difficulties creating accurate outlines due to wear or taphonomy-related damages.

The *Parapapio* specimens include MP221, MP223, and MP77. Of the three, MP221 and MP223 are identified as male *Parapapio whitei* (Williams et al. 2007), with MP77 identified as *Parapapio broomi* (Heaton 2006). All three specimens originate from the Makapansgat cave site in South Africa, which is dated to the Pliocene (Partridge 2000; Fourie et al. 2008).

1.4 Methods

1.4.1 Data Collection

To create the measurements, images were first digitized using a camera microscope system, Toupview, at 30x zoom. From that image, the occlusal surface was measured in three ways: occlusal area, buccolingual distance, and mesiodistal distance. The occlusal area is measured using a polygon-tracing tool that utilizes the placement of points to create an outline. Outlining through landmark placements and tracing of the occlusal area are the most common methods of reproducing the shape of the tooth being studied. In this study, each outline began with placing a landmark on the lingual groove, followed by placing additional landmarks incrementally at approximately 0.5mm intervals around the occlusal surface of the molar until a trace was completed.

For elliptical Fourier analysis to be effective, it requires that the shapes used in the analysis are as accurate as possible. The act of outlining involves the placement and spacing of several points along the outer perimeter of the object being outlined, with more landmarks producing a more accurate image, and fewer landmarks producing a more generalized representation of the shape. Placing points around the occlusal area creates a polygonal shape over the image that gives the measurement of the area inside the shape. Because of the potential for observer error, a measurement error study was performed for each taxon by performing the outlines several times and comparing the resulting measurements using a T test. In each instance, the difference was minimal, and the resulting shapes were not altered in any meaningful way.

The buccolingual distance was measured from inside the created outline by using a measurement tool to draw a line from the middle of the lingual side, which typically featured an indent between the protocone and hypocone, to the middle of the buccal side. Afterward, the

mesiodistal measurement was taken inside the shape by drawing a line from a central mesial extreme to a central distal extreme. Upon completing the measurements, the images were then exported into Photoshop media editing software for binarization. Exporting the image with the outline of the occlusal surface was important for creating a binarization that was accurate with the measurements. In these binarized images, the occlusal surface of the molar is colored black, and the surrounding area is colored white.



Figure 12 Example of a Parapapio, Cercocebus, and Papio occlusal outline that would be used in elliptical Fourier analysis. After measurements are taken of the molar, the occlusal outline image is binarized to capture the shape for the analysis. Parapapio and Papio molars are up to three times as large as some Cercocebus molars, but the binarized images are scale independent because elliptical Fourier analysis captures shape rather than size.

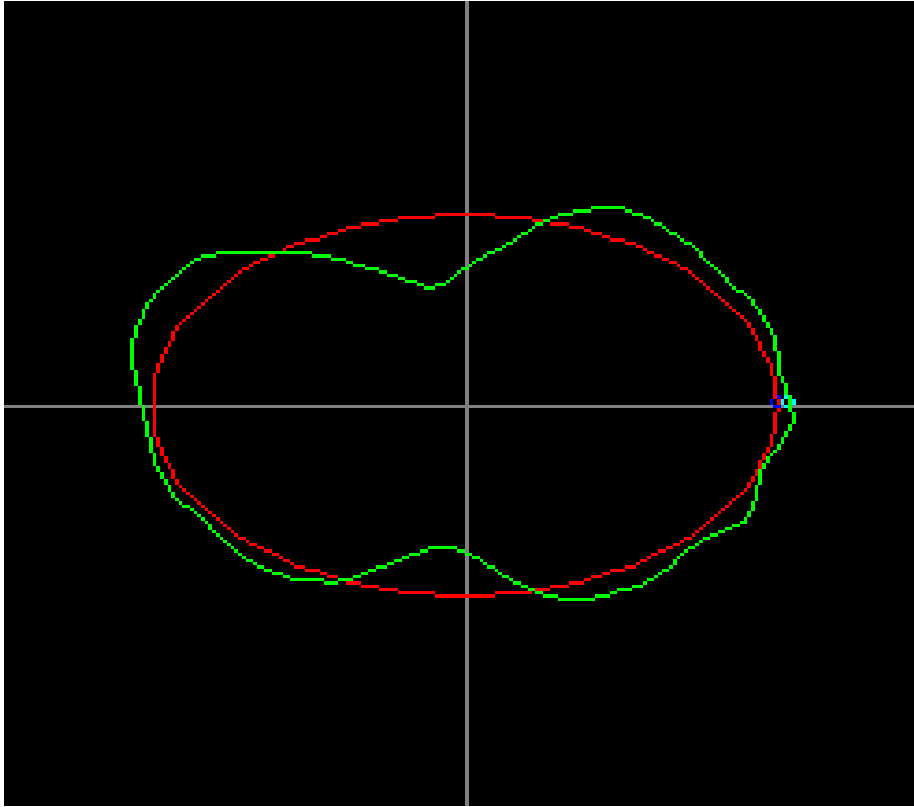


Figure 13 An example of Procrustes superimposition for elliptical Fourier analysis. The binarized molar image is reduced to the shape of the occlusal surface outline and imposed over the ellipse. The differences between the ellipse and the molar shape create the mathematical description for the principal components analysis.

1.4.2 Elliptical Fourier Analysis

With all the images binarized, they were then input into SHAPE version 2.0 which calculated the elliptical Fourier coefficients using elliptical Fourier analysis. Elliptical Fourier analysis is a method of morphometric analysis that uses the shape of an object fitted to a curve or surface to create a numerical description. This is done by comparing the outline of a chosen shape to another and then applying sine and cosine to the spatial perturbations between the overlapped shapes (Figure 12; Figure 13). The resulting sum of the comparison is a quantified expression of the shape. The resulting amplitudes of the harmonics were then reduced to principal components scores. The principal components scores were visualized within two standard deviations. For this study, the first six principal components scores were used, as the amount of variance explained for each principal components score decreases iteratively. The principal components analysis was exported into IBM SPSS statistics software, where the principal components scores were compared to create graphs that contrasted the scores.

In one study, combined generalized Procrustes superimposition and elliptical Fourier has been shown to be effective at discriminating between the first and second molars of modern humans, despite the high frequency of teeth being found separated and the morphological similarities of the first and second molars making them difficult to distinguish (Corny and Detroit 2014). Generalized Procrustes superimposition is unique in that it compares the set of landmarks to a created mean shape from the data, rather than comparing all the landmarks to an arbitrarily-selected shape. Because generalized Procrustes superimposition utilizes a changing mean shape based on the superimposed set of objects, the authors determined that 39 harmonics were sufficient while maintaining the stability of the analysis Error rates for the analysis ranged

from 1.67% to 3.33% for the upper molars, and 5.56% to 6.67% for the lower molars (Corny and Detroit 2014).

Another strength of elliptical Fourier analysis is the ability to compare shape regardless of size. Previous studies on fossil and extant primates have found Procrustes analysis to be an effective tool for comparing the shape of skull morphology across a variety of sizes (Fleagle et al. 2016). For anthropologists, elliptical Fourier analysis is especially effective due to the large variation in size exhibited in humans and non-human primate species. For the purposes of comparing *Cercocebus*, *Colobus*, *Papio*, and *Parapapio*, this is particularly useful due to the wide range of molar size differences between the taxa. While the molars of *Papio* and *Parapapio* are typically between two to three times as large as those of *Cercocebus* and *Colobus*, elliptical Fourier analysis does compare the shapes of the taxa without any needed input regarding the size of the teeth.

The ability to discern between genera of differing allometries is essential to correctly compare their morphological features. In a study performed on two different rat species, *Rattus exulans* and *Rattus tanezumi*, elliptical Fourier analysis and log shape ratios were used to compare the shape of the two species' teeth and skulls (Claude 2013). There is a large amount of intraspecific variation in rats, which can make discerning between species challenging. Despite a limited sample size of *Rattus exulans* and similarly-shaped features, 66% of the taxa were correctly reclassified through elliptical Fourier analysis. The authors admit that a more extensive data set is important for effectively discerning between taxa (Claude 2013). It was determined that analyses of shape, through Procrustes or outline methods, were much more effective at displaying differences in the species compared to shape ratio analyses and could be applied to other anatomical traits (Claude 2013).

1.4.3 Resampling

The method of resampling used in this analysis, referred to as ‘bootstrapping,’ uses replacement, meaning that the same specimen may appear in the generated data set more than once. Importantly, this method can test the accuracy of sampling distributions. Entirely new principal components scores were generated by resampling the existing principal components scores of each taxon 100 times with replacement, and then taking the mean of each set of 100 principal components scores as a newly-created specimen. After bootstrap testing resulted in intraspecific overlap between 50 to 70 attempts, this was performed 30 times per taxa to create 30 new specimens for comparison against the original data set. Creating a new data through this method reduces the impact of extreme outliers on the analysis of smaller samples.

When comparing the occlusal surfaces of molars, it is necessary to be selective about which teeth are being chosen. Due to having a diet consisting primarily of hard and tough food objects, cercopithecoid monkeys typically do exhibit a large amount of damage to their teeth as they age. Dental casts can further complicate the selection process because of casting errors. The potential for these difficulties to influence data collection give emphasis to the value of resampling. When looking at extinct taxa like *Parapapio*, this problem is often exacerbated by millions of years of post-mortem damage that can destroy the occlusal surface of the teeth altogether. Due to the limited number of *Parapapio* specimens available, combined with the ante- and post-mortem damages, resampling is a vital tool for bolstering sample numbers and creating a more robust data set for significance tests.

In an academic environment, resampling is most frequently performed with R software, which has two advantages over alternative statistical software: it is open-source, and it is platform-agnostic. Open-source software is free, accessible, and highly modifiable by user-

created modules. Some of these modules are created specifically for morphometric analysis, such as Procrustes superimposition. The advantage of being platform-agnostic means that the software and the data are not reliant on any particular operating system, which can be problematic with other alternatives as many are designed primarily for Microsoft Windows. Resampling in R is the optimal way to address concerns about sample sizes while ensuring that the data are accessible across multiple platforms.

The most effective means of resampling the taxa for elliptical Fourier analysis is to directly resample the principal components scores for comparison, rather than resampling the individual measurements. Resampled measurements cannot be used for elliptical Fourier analysis, because the shape of the object cannot be constructed from the measurements alone. It is possible that objects with similar measurements exhibit entirely different shapes. Resampling the measurements is potentially beneficial for other types of analyses or comparison, such as creating an elliptical distribution function or histogram.

2 RESULTS

2.1 Measurements

Table 1 First and second trials for the measurements of the taxa, as well as specimen labels.

Specimen	ID#	Area1	MD1	BL1	Area2	MD2	BL2
<i>CERCOCEBUS AGILIS</i>							
DSC04493 RG 6969	1	23.75	7.15	2.95	23.72	7.11	2.82
DSC04562 RG 9960	1	27.17	6.82	3.36	26.81	6.92	3.55
DSC04585 RG 10236	1	24.28	6.66	2.77	24.09	6.67	2.77
DSC04606 RG 10097	1	27.36	7.18	3.27	27.16	7.27	3.37
DSC04766 RG 8283	1	35.72	7.64	3.6	35.82	7.69	3.65
DSC04847 RG 5375	1	24.76	6.58	3.19	24.78	6.56	3.19
RG26555	1	22.03	6.8	2.85	22.04	6.78	3
RG12343	1	24.83	7.31	2.68	25.03	7.43	2.76
RG37589	1	26.36	6.74	3.3	26.39	6.81	3.28
RG8347	1	29.72	7.03	3.31	29.79	6.98	3.38
RG8380	1	33.63	6.8	3.74	33.61	6.82	3.67
<i>COLOBUS ANGOLENSIS</i>							
RG2746	2	22.44	6.72	3.27	22.37	6.72	3.36
91-060m120	2	23.83	6.28	3.21	24.03	6.27	3.26
91-060m113	2	24.24	6.16	3.36	24.21	6.26	3.36
RG13591	2	19.08	5.78	2.95	19.09	5.74	2.87
RG5637	2	20.33	6.13	3.22	20.45	6.14	3.24
RG8107	2	24.72	6.29	3.54	24.89	6.31	3.58
RG4159	2	23.5	6.18	3.24	23.68	6.07	3.38
RG10546	2	22.43	5.95	3.19	22.27	5.95	3.19
91060M118	2	24.11	6.44	3.16	24.09	6.34	3.19
91060M121	2	23.6	6.5	3.67	23.67	6.5	3.64
91060M122	2	19.37	5.65	3.28	19.32	5.56	3.18
<i>PAPIO ANUBIS</i>							
RG6025	3	95.23	12.15	6.46	95.15	12.27	6.42
RG18472	3	84.46	12.11	5.72	83.73	12.13	5.74
RG17738	3	80.46	12.1	5.87	79.61	11.96	5.9
RG9253	3	66.45	11.22	5.22	66.59	11.15	5.3
RG10416	3	90.52	12.26	5.85	91.27	12.38	5.88
RG18471	3	76.86	12.16	5.88	76.27	12.23	5.81
RG11664	3	71.89	10.53	5.87	71.31	10.52	5.86
RG18206	3	61.68	10.53	4.85	61.35	10.52	4.94
RG14450	3	71.72	10.81	5.3	72.12	10.78	5.53
RG6229	3	67.6	11.63	5.22	67.74	11.57	5.31
<i>PARAPAPIO</i>							
MP77	4	64.41	10.07	5.03	63.99	10.01	5.27
MP221	4	58.91	9.98	4.46	59.01	10.02	4.28
MP223	4	81.71	10.01	5.77	83.63	10.15	5.78

Table 2 Comparison of means for the measurements made on the first maxillary molars of the taxa. These taxa are morphologically distinct in size, as is reflected in the differences in their molar measurements.

Genera	Occlusal Area(mm ²)	Mesiodistal(mm)	Buccolingual(mm)
<i>Cercocebus</i> (n = 11)	27.22	6.98	3.20
<i>Colobus</i> (n = 11)	22.53	6.17	3.28
<i>Papio</i> (n = 10)	76.60	11.55	5.64
<i>Parapapio</i> (n = 3)	68.61	10.02	5.08

Table 3 The differences between the first and second set of measurements performed for the measurement error analysis were not found to be significant.

Measurement	Significance Value Between Trials
Occlusal Area	1.000
Buccolingual	9.888
Mesiodistal	0.879

Table 4 ANOVA results across taxa.

Measurement	F Value	P Value
Occlusal Area	135.387	< 0.001
Buccolingual	286.066	< 0.001
Mesiodistal	101.566	< 0.001

*Table 5 Tukey's Test between taxa. All measurements resulted in significantly different means between taxa except for the area measurements between *Cercocebus* and *Colobus*, and *Papio* and *Parapapio*.*

Genera Comparisons	Occlusal Area P Value	Buccolingual P Value	Mesiodistal P Value
<i>Cercocebus</i> and <i>Colobus</i>	0.418	0.002	0.928
<i>Cercocebus</i> and <i>Papio</i>	0.000	< 0.001	< 0.001
<i>Cercocebus</i> and <i>Parapapio</i>	0.000	< 0.001	< 0.001
<i>Colobus</i> and <i>Papio</i>	0.000	< 0.001	< 0.001
<i>Colobus</i> and <i>Parapapio</i>	0.000	< 0.001	< 0.001
<i>Papio</i> and <i>Parapapio</i>	0.302	< 0.001	0.151

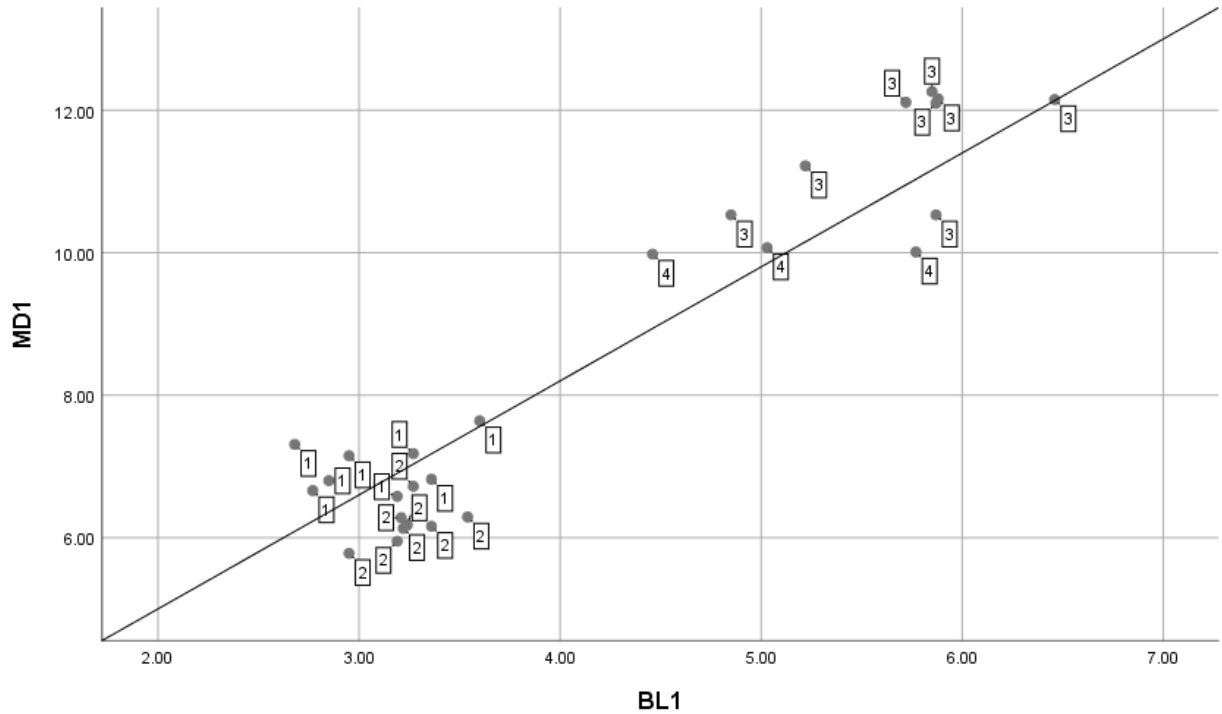


Figure 14 The linear regression of the mesiodistal and buccolingual measurements taken from the first trial. Cercopithecus and Papio are primarily above the regression line, while Colobus is mostly below the regression line. Parapapio specimens display a normal dispersion.

2.2 Analysis

2.2.1 Measurements

Cercocebus agilis was given the genus identifier 1. The average area of the occlusal surface is 27.22mm^2 , with the mesiodistal measurement averaging 6.98mm , and the buccolingual measurement averaging 3.20mm (Table 1; Table 2). The total mean percent difference between all of the occlusal area measurements for *Cercocebus* is .13%. *Colobus angolensis* is identified as genus 2 in the data (Table 1). There are no extreme observations in this group of specimens. The occlusal area averages at 22.53mm^2 , while the mesiodistal and buccolingual measurements average at 6.17mm and 3.28mm , respectively (Table 1; Table 2). The total mean percent difference for the occlusal area measurement of *Colobus* is .15%. While similar in size, the difference in width between *Cercocebus* and *Colobus* is statistically significant (Table 5). In *Papio anubis*, identified as 3 in the data, the occlusal area averages at 76.60mm^2 , while the mesiodistal measurement averages at 11.55mm and the buccolingual measurement averages at 5.64mm (Table 1). The total mean percent difference is .23%. Lastly, *Parapapio*, identified as 4, has an average occlusal surface area of 68.61mm^2 (Table 1). The mesiodistal measurements average at 10.02mm , and the buccolingual at 5.09mm . The total mean percent difference in *Parapapio* is .62%. Like *Cercocebus* and *Colobus*, the width of *Parapapio* and *Papio* molars is significantly different. The measurement error study showed no significant difference between trials (Table 3).

The bivariate plot of the mesiodistal and buccolingual lengths show that while *Cercocebus* and *Colobus* are close in size, they differ in proportion. *Cercocebus* has longer molars, while *Colobus* molars are wider. *Papio* molars are longer than they are wide, while the *Parapapio* specimens were evenly distributed, showing little mesiodistal variation but some

buccolingual variation (Figure 14). When all taxa are compared in ANOVA testing, the results indicate that they are significantly different across all measurements (Table 4).

2.2.2 Principal Components Analysis

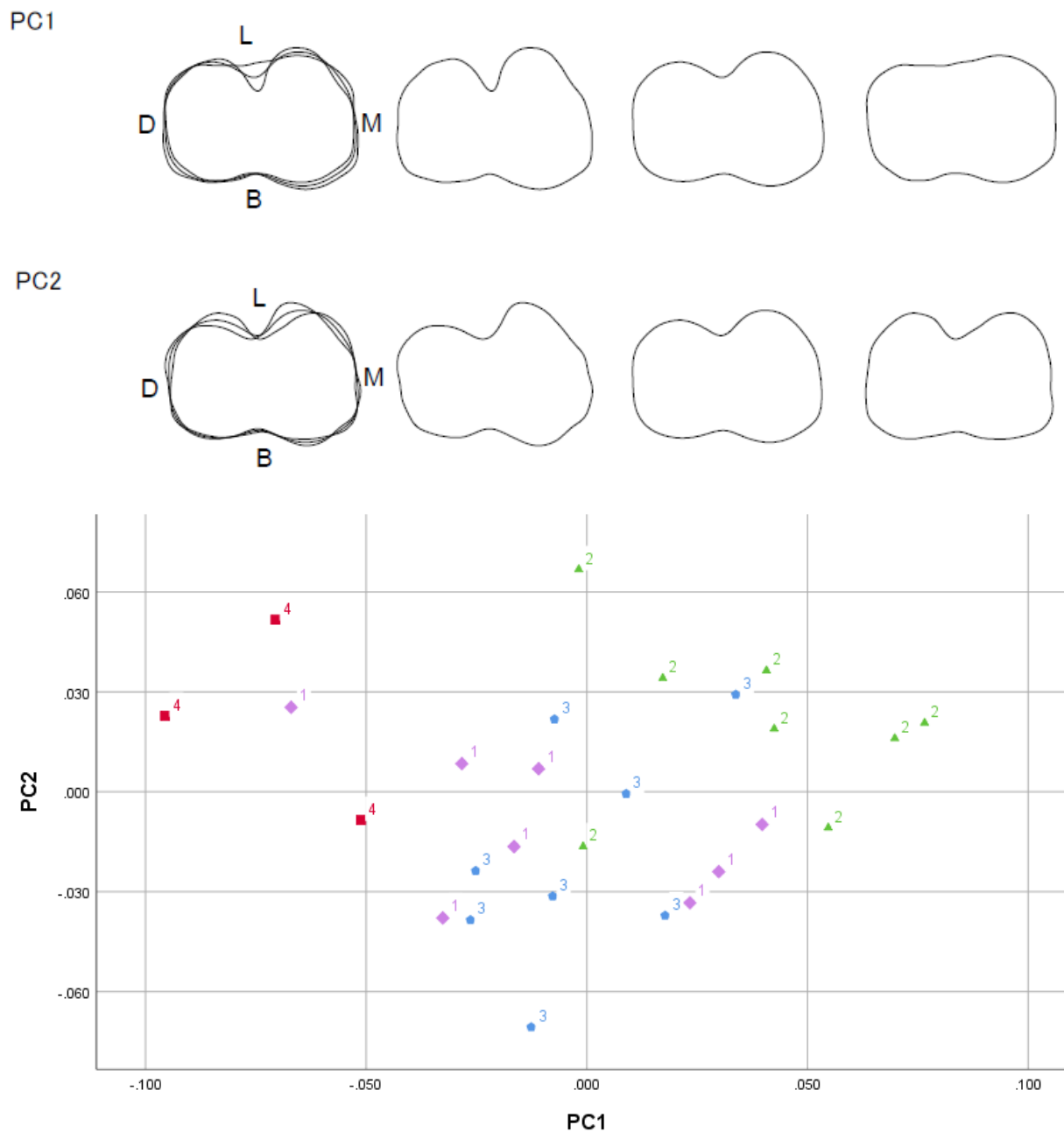


Figure 15 Visualization and graph of contrasting PC 1 and PC 2. 1 represents *Cercocebus*, 2 represents *Colobus*, 3 represents *Papio*, and 4 represents *Parapapio*.

The first principal components score explains 35% of the variation in the shape of the occlusal area, and the second principal components score explains 19.76% (Figure 15). Together, these scores explain the majority of the variation at a total of 54.76%. For PC1, the visualization shows a high amount of variation in the shape of the lingual side of the molar between the protocone and the hypocone. There is a smaller amount of variation on the buccal side, directly on the paracone and metacone. The visualization of PC2 reduces the emphasis on the groove between the protocone and hypocone and instead emphasizes the variation of those two cusps themselves. On the graph, *Cercocebus* is tightly grouped around the midpoint of PC1, and slightly below the midpoint of PC2. *Colobus* is dispersed on the positive side of PC1 and intermittently around the middle of PC2. *Papio* is clustered around the middle of PC1 and predominantly placed slightly below the midpoint of PC2. The three *Parapapio* are heavily negative on PC1 but strongly positive on PC2. Across PC1, *Parapapio* is polarized from other genera, while *Cercocebus* and *Papio* are also polarized from *Colobus*.

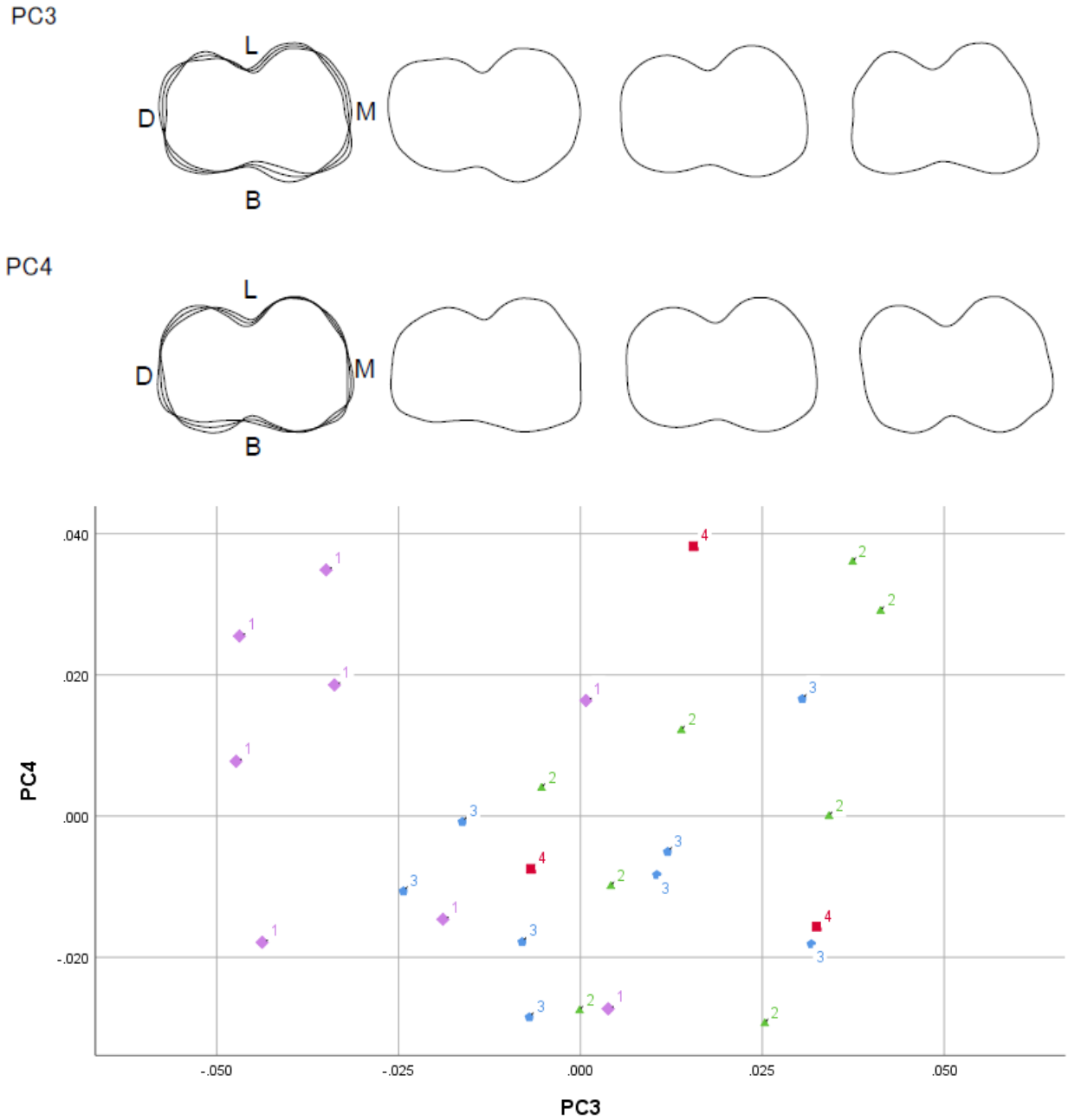


Figure 16 Visualization and graph of contrasting PC 3 and PC 4. 1 represents *Cercocebus*, 2 represents *Colobus*, 3 represents *Papio*, and 4 represents *Parapapio*.

The third and fourth PC score explain 13.92% and 8.57% of the variation, or 22.49% cumulatively (Figure 16). In total, PC scores 1 through 4 describe 77.27% of the variation. The visualization of PC3 shows differences in variation at all sides of the molar with some overlap, but the most extreme differences are seen at the mesial and buccal sides of the paracone. For PC4, the visualization is most wide-ranging at the distal end of the tooth, where both the metacone and hypocone exhibit the majority of the variation. *Cercocebus* is polarized to the negative axis of PC3, with a wide range of variation on PC4. For *Colobus*, the dispersion is largely on the positive side of PC3, but the spread across PC4 ranges to both extremes. *Papio* is widely distributed on both PC3 and PC4 but slightly distributed across the negative side of both. *Parapapio* appears to be clustered on PC3, and on the negative side of the PC4 with one outlier, MP223. *Cercocebus* and *Colobus* are largely separated from each other on opposite extremes of PC3.

The fifth and sixth PC scores explain the least amount of variation (Figure 17). PC score 5 explains 5.43% of the variation, and PC score 6 explains 3.62%, for a total 9.05% of the variation explained. Altogether, the six PC scores describe 86.33% of the variation between the molars. In the visualization, there are very few disturbances. The distal ends of both PC5 and PC6 show almost no differences. PC5 exhibits some variation on the buccal side of the molar, primarily on the paracone, as well as the mesial side of the protocone. PC6 is consistent with PC5, with fewer disturbances but those that are visible are in the same regions of the molar. The scores of PC5 and PC6 are the most tightly clustered of the three, with very little variation across PC5. However, the variation that exists is strongly negative relative to the rest of the individuals. *Cercocebus* is mainly located on the positive sides of PC5 and PC6 with a few exceptions. *Colobus* groups around 0 for PC5 but is predominantly positive on PC6. *Papio* is widely distributed on PC5 and found on both extremes of PC6, making it the most widely dispersed on that score. On PC5, *Parapapio* is the most polarized, while being the least varied on PC6. While not completely removed from the others, *Papio* and *Parapapio* are somewhat isolated from the other genera on the negative extreme of PC5.

2.2.3 Resampling and Comparison

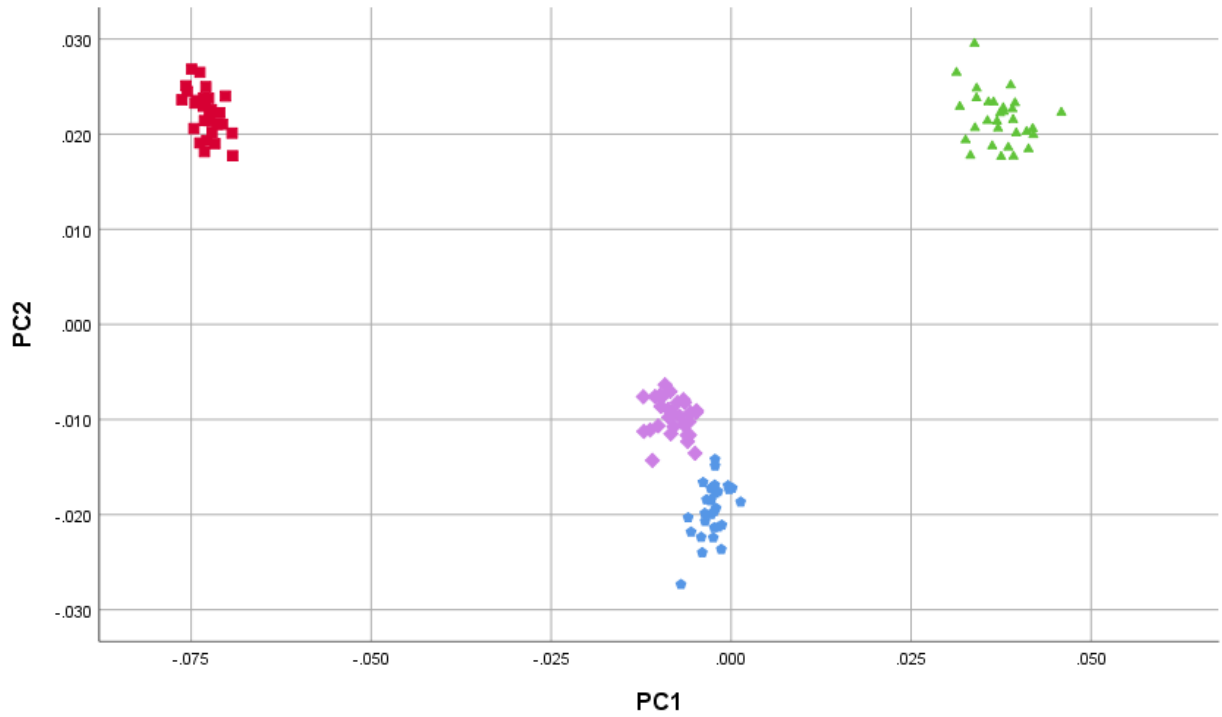


Figure 18 Graph of resampled PC1 and PC2. Papio and Cercocebus are closely grouped; Cercocebus is also the taxon in closest proximity to Parapapio

In resampled PC1, *Parapapio* and *Colobus* are located at negative and positive extremes, respectively, with *Cercocebus* slightly negative to but still clustered closely with *Papio* in the center (Figure 18). While *Cercocebus*, *Papio*, and *Colobus* remain in some proximity, *Parapapio* is mostly removed from the other three along this axis. On PC2, *Cercocebus* and *Papio* range slightly negative, but still remain close with *Cercocebus* trending slightly positive to *Papio*. *Parapapio* and *Colobus* are positive and occupy the same place on PC2, grouping between .01 and .03 for all specimens. This supports the patterns from the original PC1 and PC2, but groups the taxa more closely, whereas they were more interdispersed in the original data.

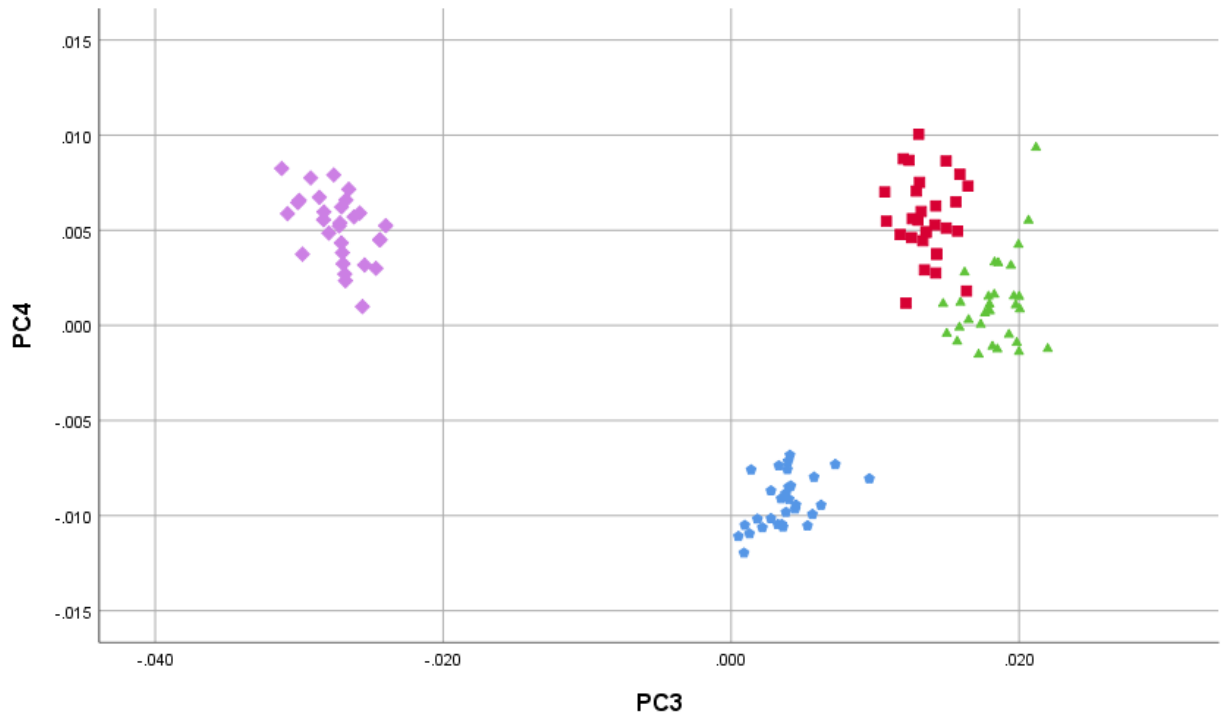


Figure 19 Graph of resampled PC3 and PC4. Parapapio and Colobus are grouped here, while Papio and Cercocebus are now separated. Cercocebus aligns with Parapapio and Colobus on PC4, while Papio is closer to Parapapio and Colobus on PC3.

Resampled PC3 continues to group *Parapapio* with *Colobus*, while now separating *Cercocebus* completely from *Papio* (Figure 19). *Colobus*, *Parapapio*, and *Papio* are positive on the axis while *Cercocebus* is strongly negative. Additionally, *Papio* is the most widely distributed on PC3. On PC4, *Cercocebus* and *Parapapio* are positive, with some *Colobus* slightly negative but still positive to *Papio*. *Colobus* is the most widely dispersed taxa on PC4, while *Papio* is the most closely clustered. While the placement of *Cercocebus* is reflective of the real data, the rest of the taxa groups are better defined in the resampled data compared to the original PC3 and PC4, which failed to separate them.

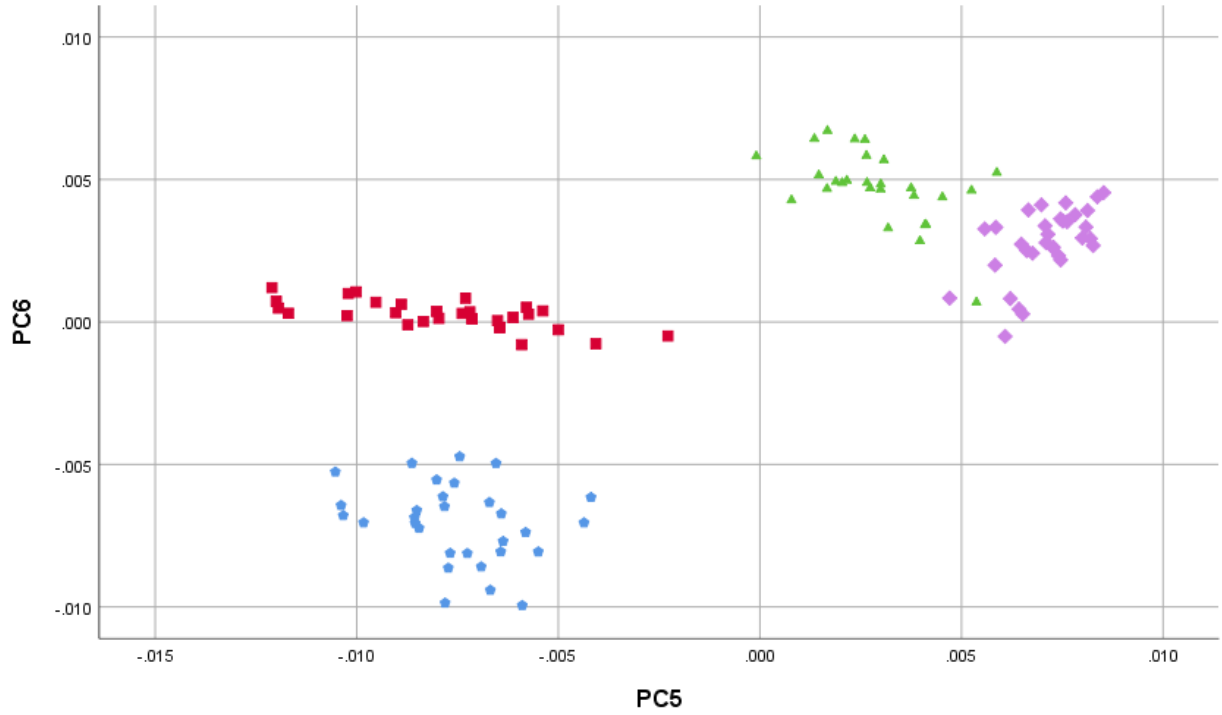


Figure 20 Graph of resampled PC5 and PC6. Parapapio clusters with Papio on PC5 and with Cercocebus and Colobus on PC6. Colobus and Cercocebus are grouped on both PC5 and PC6.

PC5 and PC6 are the most closely grouped of the data represented in the resampling, primarily due to the lower amount of variation they explain (Figure 20). Still, the taxa groups are well-defined compared to the original data. On PC5, *Papio* and *Parapapio* occupy around the same negative range, though with *Parapapio* slightly less clustered. Both *Colobus* and *Cercocebus* are positive, though *Cercocebus* is the more positive of the two taxa. On PC6, *Papio* is the most removed of the taxa and trends heavily negative, while *Parapapio* is dispersed around 0, negative to *Cercocebus* and *Colobus*, the latter of which is the most positive of the groups. The resampled groups recreate the separation of *Papio* and *Parapapio* seen in the real PC5. PC6 exhibits more defined groupings of the taxa in the resampled data compared to the original PC6 where the taxa fail to separate.

3 DISCUSSION

3.1 Separating Taxa by Elliptical Fourier Analysis

The results support the assertion that size does not significantly influence the discrimination of taxa by the shape of the molars using elliptical Fourier analysis, as the first two principal components scores explain the majority of the variation, and *Cercocebus* is grouped predominantly with *Papio* while being largely removed from *Colobus*. These results are further supported by the resampled data, which continues to group *Papio* with *Cercocebus* on PC1 and PC2, the two PC scores which represent approximately 55% of the variation, while separating *Colobus* from all taxa on PC1 but grouping it with *Parapapio* on PC2, despite *Parapapio* being more closely related to *Cercocebus* and *Papio*. The most plausible explanation for this result is that *Parapapio* and *Colobus* are being polarized due to differences with *Papio* and *Cercocebus*, rather than being grouped due to morphological similarities. Another possible, though less likely, explanation is that *Parapapio* from South Africa were more herbaceous than extant cercopithecines, consuming more C₄ plant matter like grass roots than either *Cercocebus* or *Papio*, and perhaps the molar shape of *Parapapio* is reflecting this dietary distinction. Additionally, the principal components analysis consistently grouped the male *Parapapio whitei* specimens, MP221 and MP223, in close proximity while excluding the *Parapapio broomi* specimen, MP77. This could be a result of intergeneric variation, but with the limited sample size, it is difficult to be certain. Further analysis of other *Parapapio* specimens will be needed to clarify this point.

3.2 Dental Morphology

Papio and *Parapapio* are substantially larger in all measurements compared to the other taxa, with the former being slightly larger than the latter. Additionally, *Cercocebus* is larger than

Colobus, but with some overlap of the smaller *Cercocebus* and larger *Colobus*. The mesiodistal and buccolingual measurements appear to fail at convincingly separating *Cercocebus* and *Colobus*, as both measurements are similar in length overall. However, the mesiodistally longer and buccolingually shorter molars of *Cercocebus* reflect the dietary adaptations made by *Colobus*. The pinched constriction from the groove found at the lingual side of *Cercocebus*, *Papio*, and *Parapapio* is diminished in *Colobus* as a result of their bilophodont molars, which take on a more rectangular shape to accommodate the rows of connected cusps associated with a folivorous diet. This rectangular shape is also maintained by the decreased relative size difference of the protocone and hypocone in *Colobus*. The hypocone has been found to be highly variable in primate dentition, especially on the first molar, and is sometimes not present at all (Turner et al. 1991).

The overall shape of the molars is very similar between *Cercocebus* and *Papio*, most notably on the lingual side of the molar, as seen in PC1 and PC2 (Figure 8). PC1, which reflects the variation of the lingual groove, separates *Colobus* and *Parapapio* at opposite extremes. This is representative of the reduced lingual groove in *Colobus*, and perhaps a deeper groove in *Parapapio*. *Parapapio* and *Colobus* do share similar scores along PC2, though, indicating that the lingual cusps are similar in shape despite the differences in the lingual groove size. On PC3, which represents the variation at the mesial and buccal aspects of the molar, *Parapapio* and *Colobus* are clustered together again. The former are grouped with *Cercocebus* on PC4, suggesting a similar shape on the distal end of the molar, specifically on the buccal side of the metacone. *Papio* and *Parapapio*, as well as *Colobus* and *Cercocebus*, are grouped on PC5 indicating some slight similarities in the shape of the protocone and paracone closer to the mesial surface of the molar. Additionally, *Colobus* and *Cercocebus*, and to a lesser extent, *Parapapio*,

are grouped on PC6, which shows small amounts of variation in the buccal groove, with *Papio* as the outlier.

3.3 Implications for Cercopithecoid Phylogeny

3.3.1 *Procercocebus* and *Parapapio*

While the results of this research do not contradict the existing cladistics of papionins, they are interesting in context with recent developments relating to the separation of *Papio* and its clade from the *Cercocebus/Mandrillus* clade. As of 2007, *Parapapio antiquus* from the Taung site has been reclassified as representative of a new sister genus to *Cercocebus* called *Procercocebus*. It has been suggested that the characteristics of *Procercocebus* can still be found in the extant *Cercocebus torquatus*, which has retained cranial morphology similar to that of *Procercocebus* (Gilbert 2007). *Cercocebus torquatus* is also notable in its resemblance to *Papio* and affinity for terrestrial behavior compared to other *Cercocebus* species (Szalay and Delson 1979). Since this distinction was established, further analysis of postcranial remains believed to have belonged to *Parapapio* and *Procercocebus* have reinforced the establishment of the *Procercocebus* genus, with the discovery that the humerus of *Procercocebus antiquus* exhibits characteristics associated with terrestrial locomotion and closely resembles that of the closest living relative of *Cercocebus*, *Mandrillus* (Gilbert et al. 2016).

If *Procercocebus antiquus* is not ancestral to *Cercocebus*, the similar molar shape of *Papio* to *Cercocebus* represented in PC1 and PC2 raises questions about the evolution of dietary adaptations as being reflected in the molar shape of papionins. One of the defining adaptations of the *Procercocebus/Mandrillus/Cercocebus* clade is the increased dependence on the premolars for the processing of hard food objects, potentially decreasing selective pressures on the

morphology of the molars and causing a retention of the ancestral molar shape shared with *Parapapio* and *Papio* (Gilbert 2013). This hypothesis is further supported by the identification of *Papio anubis* as being one of two *Papio* taxa that retain the greatest amount of ancestral craniodental morphologies, indicating that it may also reflect an ancestral molar shape that evolved after the emergence of *Parapapio* but before the divergence of *Procercocebus* approximately 1.5 to 2 million years ago (Gilbert 2007; Gilbert et al. 2018). The inclusion of other extant papionin genera such as *Macaca* and *Mandrillus* could potentially elucidate the extent to which papionin occlusal molar shape has differentiated across diets since the Pliocene.

3.3.2 *Parapapio* species: one, two, three?

It is important to consider that *Parapapio* species likely exhibited locomotive, size, and dietary differences due to occupying a variety of niches (Fourie et al. 2008). This complicates the grouping and comparison of potentially multiple *Parapapio* species in this study. However, the differences between Makapansgat *Parapapio* have been largely associated with differences between sex, not species. *Parapapio whitei*, *Parapapio broomi*, and *Parapapio jonesi* are typically discriminated by molar size due to the morphological similarities of the taxa, with *Parapapio whitei* being the largest, *Parapapio jonesi* being the smallest, and *Parapapio broomi* overlapping somewhat with *Parapapio whitei* in the center (Freedman and Stenhouse 1972; Fourie et al. 2008). Despite a consistent molar morphology between the taxa, isotopic analysis indicates that *Parapapio broomi* had a mixed C₃ diet, while *Parapapio whitei* and *Parapapio jonesi* had a mixed C₄ diet (Fourie et al. 2008). This is not surprising as papionins are known for their dietary flexibility as generalist consumers (Codron et al. 2005). Because of the morphological similarities, the separation of these taxa as three distinct species has yet to be convincingly established, and the possibility that these taxa represent one species remains

entirely possible based on current morphological studies (Fourie et al. 2008). For these reasons, the inclusion of all three Makapansgat *Parapapio* is important. The elliptical Fourier analysis repeatedly distinguished MP77, a specimen attributed to *Parapapio broomi*, as being at least somewhat distinct in shape (Heaton 2006). This supports the hypothesis that elliptical Fourier analysis can be used to identify differences between even closely related taxa based on molar shape alone. With the inclusion of more *Parapapio* taxa, the potential of this promising method for identifying species that are difficult to discriminate could be expanded upon for future analyses.

4 CONCLUSION

Despite the limited sample size, the elliptical Fourier analysis successfully separated the taxa by molar occlusal shape, grouping the extant cercopithecines, *Papio* and *Cercocebus*, despite being closer in size to *Parapapio* and *Colobus*, respectively. These are promising findings on the validity of using elliptical Fourier analysis on molar occlusal surface areas to classify primate taxa, which can perhaps strengthen the argument of their phylogenetic position, provided enough specimens to create meaningful analyses.

The analysis also found that the majority of the variation takes place on the lingual side of the tooth on the protocone and hypocone, as well as the lingual groove that separates the two cusps. On PC2, PC3, and PC4 of the resampled data, *Parapapio* appears to share some morphological similarities in the reduced shape of the lingual groove with *Colobus*, perhaps reflecting its increased reliance on folivory compared to *Papio* and *Cercocebus*.

The two *Parapapio whitei* specimens consistently clustered together in the principal components analysis, repeatedly isolating *Parapapio broomi* on its own or placing it with other taxa. Current knowledge of *Parapapio* molar morphology indicates that the best method of distinguishing between *Parapapio* species is by molar size, but these differences are miniscule, and some anthropologists have posited the possibility that the *Parapapio whitei*, *Parapapio broomi*, and *Parapapio jonesi* are one species. The possibility that elliptical Fourier analysis might be capable of identifying *Parapapio* at the species level is worth exploring. While more testing is required to validate the findings of this analysis, this method could be a potential alternative to discerning *Parapapio* species without relying solely on the size of the molars. This project could be further developed with the inclusion of more *Parapapio* specimens, other fossil

taxa like *Cercopithecoides*, and additional extant taxa such as *Mandrillus* and *Cercocebus torquatus*.

REFERENCES

- Buck, L. T., Stock, J. T., & Foley, R. A. (2010). Levels of intraspecific variation within the catarrhine skeleton. *International Journal of Primatology*, *31*(5), 779–795.
- Claude, M. (2013). Log-shape ratios, Procrustes superimposition, elliptic Fourier analysis: three worked examples in R. *Hystrix*, *24*(1), 94–102.
- Codron, D., Luyt, J., Lee-Thorp, J. A., Sponheimer, M., De Ruiter, D., & Codron, J. (2005). Utilization of savanna-based resources by Plio-Pleistocene baboons. *South African Journal of Science*, *101*(5–6), 245–248.
- Corny, J., & Déroit, F. (2014). Technical note: anatomic identification of isolated modern human molars: testing Procrustes aligned outlines as a standardization procedure for elliptic Fourier analysis. *American Journal of Physical Anthropology*, *153*(2), 314–322.
- Delson, Eric. (1984). Cercopithecoid biochronology of the African Plio-Pleistocene: correlations among eastern and southern hominid-bearing localities. *Courier Forschungsinstitut Senckenberg* *69*, 199–218.
- Delson, E., Terranova, C., Jungers, W., Sargis, E., Jablonski, N., & Dechow, P. (2000). Body mass in cercopithecidae (Primates, Mammalia): Estimation and scaling in extinct and extant taxa. In *Anthropological Papers of the American Museum of Natural history* (Vol. 83).
- El-Zaatari, S., Grine, F. E., Teaford, M. F., & Smith, H. F. (2005). Molar microwear and dietary reconstructions of fossil cercopithecoidea from the Plio-Pleistocene deposits of South Africa. *Journal of Human Evolution*, *49*(2), 180–205.
- Fleagle, J. G., Gilbert, C. C., & Baden, A. L. (2016). Comparing primate crania: the importance of fossils. *American Journal of Physical Anthropology*, *161*(2), 259–275.
- Fourie, N. H., Lee-Thorp, J. A., & Ackermann, R. R. (2008). Biogeochemical and craniometric investigation of dietary ecology, niche separation, and taxonomy of Plio-Pleistocene cercopithecoids from the Makapansgat limeworks. *American Journal of Physical Anthropology*, *135*, 121–135.
- Freedman, L., & Stenhouse, N. S. (1972). The *Parapapio* species of Sterkfontein, Transvaal, South Africa. *Paleontologica Africana*, (14), 93–111.
- Frost, S. R., Gilbert, C. C., Pugh, K. D., Guthrie, E. H., & Delson, E. (2015). The hand of *Cercopithecoides williamsi*: earliest evidence for thumb reduction among colobine monkeys. *PLoS ONE*, *10*(5), 1–18.
- Gilbert, C. C. (2013). Cladistic analysis of extant and fossil African papionins using craniodental data. *Journal of Human Evolution*, *64*(5), 399–433.

- Gilbert, C. C. (2007). Craniomandibular morphology supporting the diphyletic origin of Mangabeys and a new genus of the *Cercocebus/Mandrillus* clade, *Procercocebus*. *Journal of Human Evolution*, 53(1), 69–102.
- Gilbert, C. C., Frost, S. R., Pugh, K. D., Anderson, M., & Delson, E. (2018). Evolution of the modern baboon (*Papio hamadryas*): A reassessment of the African Plio-Pleistocene record. *Journal of Human Evolution*, 122, 38–69.
- Gilbert, C. C., Frost, S. R., & Strait, D. S. (2009). Allometry, sexual dimorphism, and phylogeny: a cladistic analysis of extant African papionins using craniodental data. *Journal of Human Evolution*, 57(3), 298–320.
- Gilbert, C. C., Takahashi, M. Q., & Delson, E. (2016). Cercopithecoid humeri from Taung support the distinction of major papionin clades in the South African fossil record. *Journal of Human Evolution*, 90, 88–104.
- Gommery, D., Thackeray, J. F., S negas, F., Potze, S., & Kgasi, L. (2008). The earliest primate (*Parapapio* sp.) from the Cradle of Humankind World Heritage Site (Waypoint 160, Bolt's Farm, South Africa). *South African Journal of Science*, 104(9–10), 405–408.
- Heaton, J. L. (2006). Taxonomy of the Sterkfontein fossil Cercopithecinae: The Papionini of Members 2 and 4 (Guateng, South Africa). Indiana University, Bloomington.
- Hlusko, L. J., Do, N., & Mahaney, M. C. (2006). Genetic correlations between mandibular molar cusp areas in baboons. *Yearbook of Physical Anthropology*, 49(December 2006), 2–48.
- Hlusko, L. J., Weiss, K. M., & Mahaney, M. C. (2002). Statistical genetic comparison of two techniques for assessing molar crown size in pedigreed baboons. *American Journal of Physical Anthropology*, 117(2), 182–189.
- Monson, T. A., & Hlusko, L. J. (2014). Identification of a derived dental trait in the Papionini relative to other Old World monkeys. *American Journal of Physical Anthropology*, 155(3), 422–429.
- Partridge, T. C. (2000). "Hominid-bearing cave and Tufa deposits." *Oxford Monographs on Geology and Geophysics* 40: 100-130.
- Pugh, K. D., & Gilbert, C. C. (2018). Phylogenetic relationships of living and fossil African papionins: combined evidence from morphology and molecules. *Journal of Human Evolution*, 123, 35–51.
- Reed, K. E. (1997). Early hominid evolution and ecological change through the African Plio-Pleistocene. *Journal of Human Evolution*, 32(2–3), 289–322.
- Strasser, E., & Delson, E. (1987). Cladistic analysis of cercopithecoid relationships. *Journal of Human Evolution*, 16(1), 81–99.

- Turner II, C., Nichol, C., & Richard, S. (1991). Scoring procedures for key morphological traits of the permanent dentition: The Arizona State University Dental Anthropology System. *Advances in Dental Anthropology*, (January 1991), 13–31.
- Szalay, F., and E. Delson. Evolutionary history of the primates. San Diego, CA: Academic Press Inc., 1979.
- Williams, F. L. (2014). Dietary reconstruction of Pliocene *Parapapio whitei*. *Folia Primatologica*, 84, 21–37.
- Williams, F. L., Ackermann, R. R., & Leigh, S. R. (2007). Inferring Plio-Pleistocene Southern African biochronology from facial affinities in *Parapapio* and other fossil papionins. *American Journal of Physical Anthropology*, 132, 163–174. <https://doi.org/10.1002/ajpa>
- Williams F. L., and E. Geissler. (2014) Reconstructing the diet and paleoecology of Plio-Pleistocene *Cercopithecoides williamsi* from Sterkfontein, South Africa. *Palaios*, 29, 483-494.
- Williams, F. L., & Patterson, J. W. (2010). Reconstructing the paleoecology of Taung, South Africa from low magnification of dental microwear features in fossil primates. *Palaios*, 25(7), 439–448.